Front. Phys. 11(6), 117407 (2016)
DOI 10.1007/s11467-016-0579-0

REVIEW ARTICLE

Applications of the conformal transformation method in studies of composed superconducting systems

Mateusz Krzyzosiak[1,*], Ryszard Gonczarek[2,†], Adam Gonczarek[3,‡], Lucjan Jacak[2,#]

[1] *University of Michigan–Shanghai Jiao Tong University Joint Institute, 800 Dongchuan Rd., Shanghai 200240, China*
[2] *Faculty of Fundamental Problems of Technology, Wrocław University of Technology, Wybrzeże Wyspiańskiego 27, 50-370 Wrocław, Poland*
[3] *Faculty of Computer Science and Management, Wrocław University of Technology, Wybrzeże Wyspiańskiego 27, 50-370 Wrocław, Poland*
Corresponding authors. E-mail: [*] m.krzyzosiak@sjtu.edu.cn, [†] ryszard.gonczarek@pwr.edu.pl, [‡] adam.gonczarek@pwr.edu.pl, [#] lucjan.jacak@pwr.edu.pl
Received March 4, 2016; Accepted March 29, 2016

A framework for analytical studies of superconducting systems is presented and illustrated. The formalism, based on the conformal transformation of momentum space, allows one to study the effects of both the dispersion relation and the structure of the pairing interaction in two-dimensional anisotropic high-T_c superconductors. In this method, the number of employed degrees of freedom coincides with the dimension of the momentum space, which is different compared to that in the standard Van Hove scenario with a single degree of freedom. A new function, the kernel of the density of states, is defined and its relation to the standard density of states is explained. The versatility of the method is illustrated by analyzing coexistence and competition between spin-singlet and spin-triplet order parameters in superconducting systems with a tight-binding-type dispersion relation and an anisotropic pairing potential. Phase diagrams of stable superconducting states in the coordinates η (the ratio of hopping parameters) and n (the carrier concentration) are presented and discussed. Moreover, the role of attractive and repulsive on-site interactions for the stability of the s-wave order parameter is explained.

Keywords high-temperature superconductivity, conformal transformation, pairing symmetry, critical temperature

PACS numbers 74.20.Rp, 74.25.Dw, 74.62.Yb, 74.20.Fg

Contents

1 Introduction

During the last three decades, high-T_c superconducting systems have been one of the most actively studied systems in condensed matter physics, both theoretically and experimentally. This is due to their huge potential in applications that span over a wide spectrum — from energy storage systems to quantum information processing. The new generation superconductors, such as copper-oxides, where charge carriers are effectively confined within the CuO_2 planes, are usually described as quasi-two-dimensional (quasi-2D) systems of fermions [1–7]. This is due to the characteristic, strongly anisotropic, layered structure of these materials with the symmetry of the CuO_2 planes characterized by the point group C_{4v} [8–12]. Currently, various approaches

are used to explain the different properties of new generation superconductors, including those with high critical temperatures [13, 14]. In most of these proposals, a single microscopic mechanism responsible for high-T_c superconductivity is assumed, although this mechanism has not been equivocally identified yet. Some of the recent ideas include a mechanism based on coupling through electron-electron interaction [15], spin exchange [16, 17], and a modified phonon-mediated mechanism [18, 19] proposed by Anderson [20, 21] and based on the concept of resonating valence bond states. On the other hand, in all of these approaches, whatever the mechanism is, it leads to the formation of Cooper pairs.

A common feature of all new generation superconducting materials, in particular those with the highest critical temperature, is not only their highly anisotropic and quasi-2D structure, but also a non-trivial dispersion relation characterizing one-particle excitations. Therefore, any theoretical approach that aims at providing an effective framework to study novel superconducting systems should be able to incorporate these features at a very fundamental level.

In Landau's theory of Fermi liquids [22, 23], one assumes that the microscopic properties of a system of strongly interacting particles can be mapped onto a gas of elementary excitations (Landau quasi-particles), with an appropriate distribution function depending on the quasi-particle energy. Additionally, there is a correspondence between the Fermi-liquid and Fermi-gas energy levels, since particles gradually changes into quasi-particles with specified energies as the interaction is being turned on slowly. Consequently, the number of quasi-particles is equal to the number of particles. However, the energy of the system is not simply the sum of energies of quasi-particles defined this way. Instead, the energy is a functional of their distribution function. For an infinitesimal change of the quasi-particle distribution function, the change in the total energy (per unit volume) is $\delta E = \int \varepsilon \delta n \mathrm{d}\tau$, where $\delta\tau = \mathrm{d}p_x \mathrm{d}p_y \mathrm{d}p_z/(2\pi\hbar)^3$. The quantity $\varepsilon(\boldsymbol{p}, \boldsymbol{\sigma}) = \delta E/\delta n(\boldsymbol{p}, \boldsymbol{\sigma})$ is the variational derivative of the energy E with respect to the distribution function n and can be considered the Hamiltonian of one added quasi-particle with a definite momentum and spin in a self-consistent field. On the other hand, in Landau's Fermi-liquid theory, the second variational derivative defines a quasi-particle interaction, the so-called Fermi-liquid interaction, which is responsible, among other things, for renormalization of the effective mass.

In the developed Landau theory, it has been assumed that the inclusion of an inter-particle interaction, which transforms a Fermi gas into a Fermi liquid, cannot change the symmetry of the system. Since the system of non-interacting fermions is isotropic, the same symmetry has to be inherited by the Fermi liquid. The assumption implies an extremely drastic limitation of possible fermion systems to which the Fermi liquid theory can be applied. In order to extend the application scope of the theory, we assume that the symmetry of the system undergoes a slow modification from isotropic to anisotropic, while the interaction is being turned on slowly (adiabatically). This procedure results in the formation of an anisotropic system for which the reciprocal anisotropic space with a non-parabolic one-particle excitation spectrum can be constructed. To reach the ultimate goal of extending the application scope of the theory, we postulate that the reciprocal (momentum) space corresponding to the anisotropic system can be transformed into an isotropic form with a parabolic (Landau) quasi-particle spectrum. However, all interaction effects that would lead to the anisotropic reciprocal space and non–parabolic energy spectrum are now included by means of an additional scalar field modifying the size of the quantum-mechanical states. This new scalar field is imposed on the isotropic reciprocal space. It is worth emphasizing that the traditional approach is entirely equivalent to the postulated one. In addition, we would like to emphasize, once again, that the complete information about interactions and symmetry of the system is contained in the introduced scalar field imposed on the momentum space. The method proves to be a very effective tool in studies of new-generation superconducting systems. In particular, it may be used, as we will show later in the present paper, to study the symmetry of the order parameter implied by the structure of the pairing potential and its group-theoretical properties [9–11, 24].

The paper is organized as follows: In Section 2 we introduce the general idea of the conformal transformation method. The effectiveness of the method is illustrated with both analytical and numerical results in Section 3, where the formalism is applied to study the problem of coexistence and mutual competition between stable spin-singlet and spin-triplet superconducting states, within both a BCS-type and a tight-binding approach. The paper concludes with a brief summary in Section 4.

2 Conformal transformation method

Because our primary interest area is in new-generation superconducting systems, we present the conformal transformation method in a formulation that can be directly applied to such quasi-2D and highly anisotropic systems [24, 25]. The mathematical foundations of the method and its detailed discussion in a more general setting were presented in Ref. [26].

2.1 Transformation of the reciprocal space

Let us consider an effective single-band model with a one-particle dispersion relation, a differentiable function of the momentum $\boldsymbol{p}$, which can be written in the form

$\xi = \xi(p_1, p_2)$, where the momentum vector is of the form $\boldsymbol{p} = p_1\boldsymbol{e}_1 + p_2\boldsymbol{e}_2$. We also assume that the dispersion relation has been renormalized by means of the mass operator, so that it includes all two-particle interactions in the particle-hole channel self-consistently. The unit vectors $\boldsymbol{e}_1$ and $\boldsymbol{e}_2$ form a basis of the momentum space, so that they are also basis vectors of the reciprocal CuO plane. The Fermi surface (line) is defined by the equation $\xi(\boldsymbol{p}) - \mu(0) = 0$, where $\mu(0)$ is the chemical potential at $T = 0$.

For an anisotropic system with a parallelogram-like reciprocal lattice the basis $\boldsymbol{e}_1$, $\boldsymbol{e}_2$ is not orthonormal. Performing a linear (orthonormal) transformation $\boldsymbol{D}$, described by a 2×2 matrix, which keeps the topology of the reciprocal planar lattice, the momentum space can be transformed in such a way that in the new space with the orthonormal basis $\boldsymbol{f}_1$, $\boldsymbol{f}_2$, where $\boldsymbol{f}_i = \boldsymbol{D}_{i1}\boldsymbol{e}_1 + \boldsymbol{D}_{i2}\boldsymbol{e}_2$, the reciprocal lattice becomes a square one. In this transformed space, the vector $\boldsymbol{p} = p_1\boldsymbol{e}_1 + p_2\boldsymbol{e}_2$ is replaced by the equivalent vector $\boldsymbol{p}' = p_1\boldsymbol{f}_1 + p_2\boldsymbol{f}_2$. Since $\boldsymbol{p}' = p_1'\boldsymbol{e}_1 + p_2'\boldsymbol{e}_2$, the introduced components satisfy the relation $p_i = \boldsymbol{D}_{1i}^{-1}p_1' + \boldsymbol{D}_{2i}^{-1}p_2'$, where $\boldsymbol{D}^{-1}$ denotes the inverse matrix. Now, the dispersion relation as a function of the momentum components p_1', p_2', determined in the orthonormal system, reads

$$\xi = \xi(\boldsymbol{D}_{11}^{-1}p_1' + \boldsymbol{D}_{21}^{-1}p_2', \boldsymbol{D}_{12}^{-1}p_1' + \boldsymbol{D}_{22}^{-1}p_2').$$

Hereafter, we assume that the particle energy in the dispersion relations is measured from the Fermi level. Then, the equation $\xi = \text{const}$ defines equi-energy lines (in particular, for $\xi = 0$, it defines the Fermi line). The shape of these lines can be quite arbitrary, although it should always reflect the symmetry of the system. Moreover, it implies that we must not treat this system of fermions as a Landau Fermi liquid. On the other hand, we need to remember that after the transformation $\boldsymbol{D}$, summation or integration in the new coordinate system requires including the Jacobian of the form

$$J(\boldsymbol{p}') = \left|\frac{\partial p_i}{\partial p_j'}\right|,$$

which is for the time being constant, and $J(\boldsymbol{p}') = \det(\boldsymbol{D}^{-1})$. Considering an anisotropic system, in which the basis vectors of its reciprocal 2D lattice $\boldsymbol{e}_1$, $\boldsymbol{e}_2$ are not orthonormal and they are not of the same length, we may assume that $|\boldsymbol{e}_1| = 1$. Then the orthonormal transformation is represented by the following matrix

$$\boldsymbol{D} = \begin{pmatrix} 1 & 0 \\ -\cot\alpha & \frac{1}{|\boldsymbol{e}_2|\sin\alpha} \end{pmatrix},$$

where α is the angle between the vectors $\boldsymbol{e}_1$ and $\boldsymbol{e}_2$. Now, the Jacobian reads $J(p_1', p_2') = |\boldsymbol{e}_2|\sin\alpha$. Eventually, after employing the above transformation we have at our disposal a system with an orthonormal basis $\boldsymbol{f}_1$ and $\boldsymbol{f}_2$ such that $|\boldsymbol{e}_1| = |\boldsymbol{f}_1| = |\boldsymbol{f}_2|$.

For instance, if the dispersion relation is of the parabolic form in the initial system, *i.e.*,

$$\xi(p_1, p_2) = \frac{1}{2m^*}(p_1^2 + p_2^2) - \mu,$$

where m^* denotes the effective mass and μ is the chemical potential, then in the transformed system

$$\xi(p_1', p_2') = \frac{1}{2m^*}[(p_1')^2 + 2p_1'p_2'|\boldsymbol{e}_2|\cos\alpha + (p_2')^2|\boldsymbol{e}_2|^2] - \mu.$$

After a rotation of the coordinate system by the angle $\beta = \frac{1}{2}\arctan\left(\frac{2|\boldsymbol{e}_2|\cos\alpha}{1-|\boldsymbol{e}_2|^2}\right)$ it reduces to a more symmetric, simplified, and equivalent form

$$\xi(p_1', p_2') = \frac{1}{2m_1}(p_1')^2 + \frac{1}{2m_2}(p_2')^2 - \mu, \tag{1}$$

where m_1 and m_2 are some mass-parameters, whose precise definitions are omitted. The Jacobian of any rotation of a coordinate system is always equal to 1. Thus, in this new Cartesian coordinate system the equi-energy lines are concentric ellipses.

Hence, the increase in the symmetry of the coordinate system is followed by a change of the form of the dispersion relation, which can now become more complicated. Therefore, the symmetry properties of the system, which are inherited from the crystal lattice symmetry, can be transferred into the dispersion relation.

2.2 Generalized conformal transformation of the reciprocal space

Now, our intention is to construct a new orthonormal 2D space in which ξ stands for one of the coordinate axes (an outline of a more general discussion is presented in Appendix A). Since $\nabla\xi$ is always perpendicular to the equi-energy lines, the following condition for the gradient direction has to be fulfilled:

$$\frac{\mathrm{d}p_1}{\partial\xi/\partial p_1} = \frac{\mathrm{d}p_2}{\partial\xi/\partial p_2}. \tag{2}$$

On the other hand, by virtue of Picard's theorem, we state that the solution of the differential equation

$$\frac{\mathrm{d}p_1}{\mathrm{d}p_2} = \frac{\partial\xi/\partial p_1}{\partial\xi/\partial p_2}$$

always exists and is a one-parameter family of integral curves $\phi = \phi(p_1, p_2)$, where the curves $\phi(p_1, p_2) = C$ are called isoclines. Note that defining the Pfaff's differential form

$$D\Xi(p_1, p_2) = -\frac{\partial\xi}{\partial p_2}\mathrm{d}p_1 + \frac{\partial\xi}{\partial p_1}\mathrm{d}p_2,$$

Eq. (2) can be read as Pfaff's equation $D\Xi(p_1, p_2) = 0$. Pfaff's equation of two independent variables always has an integrating factor $\gamma = \gamma(p_1, p_2)$, such that

$\gamma(p_1,p_2)D\Xi(p_1,p_2) = d\phi(p_1,p_2)$ is a total differential. Thus,

$$-\gamma(p_1,p_2)\frac{\partial\xi}{\partial p_2} = \frac{\partial\phi}{\partial p_1}, \quad \gamma(p_1,p_2)\frac{\partial\xi}{\partial p_1} = -\frac{\partial\phi}{\partial p_2}, \tag{3}$$

and hence the gradients $\nabla\xi$ and $\nabla\phi$, defining perpendicular directions to the equi-energy curves and isoclines, respectively, obey the condition

$$\nabla\xi\cdot\nabla\phi = \frac{\partial\xi}{\partial p_1}\frac{\partial\phi}{\partial p_1} + \frac{\partial\xi}{\partial p_2}\frac{\partial\phi}{\partial p_2} = 0,$$

which ensures that the new 2D system of curvilinear coordinates (ξ,ϕ) is orthogonal. In general, the coordinate ξ, which is the particle's energy, can vary in the conduction band, while the range of the coordinate ϕ can be chosen arbitrarily and can be infinite. However, we can formally replace ϕ by the angular coordinate of the polar coordinate system φ by using trigonometric functions. Then, the range of the new coordinate becomes finite. Note that for a function $\varphi = \varphi(\phi)$ we have the relation

$$\nabla\varphi = \frac{\mathrm{d}\varphi}{\mathrm{d}\phi}\nabla\phi,$$

which ensures that the coordinate system (ξ,φ) is also orthogonal, since $\nabla\xi\cdot\nabla\varphi = 0$. Moreover, employing the symmetry of the system, which is directly reflected in the form of the dispersion relation, we can limit our consideration to the representative region of the (p_1,p_2)-plane, and the range of the angular coordinate φ can be settled in regard to the full rotation of the plane, i.e., $0 \le \varphi < 2\pi$. Then we can assume that locally, in separated regions of the (p_1,p_2)-plane, we can derive p_1 and p_2 as functions of ξ and φ, because both functions $\xi(p_1,p_2)$ and $\varphi(p_1,p_2)$ are differentiable. On the other hand, we emphasize that the analytical forms of p_1 and p_2 as functions ξ and ϕ or φ can be derived merely for a few specific forms of the particle's energy, nevertheless they can always be found numerically. Therefore, the present method allows us to transform the 2D Cartesian coordinate system (p_1,p_2) into a specific curvilinear orthogonal coordinate system (ξ,ϕ), employing given $\xi = \xi(p_1,p_2)$ and derived $\phi = \phi(p_1,p_2)$ relations.

In the standard formulation, the conformal mapping is given by a single-valued complex analytic function, where its real and imaginary parts define equi-energy curves and isoclines, respectively, which satisfy the Cauchy-Riemann conditions. Since we do not require that

$$\frac{\partial\xi}{\partial p_1} = \frac{\partial\phi}{\partial p_2}, \quad \frac{\partial\xi}{\partial p_2} = -\frac{\partial\phi}{\partial p_1},$$

and conditions of the Cauchy–Riemann type are satisfied only if $\gamma(p_1,p_2) \equiv 1$, we maintain that the present formalism constitutes a generalization of the conformal transformation, contrary to the standard conformal transformation where these conditions must be fulfilled. Note that, in the present formalism, the function $\phi(p_1,p_2)$ is not given but is derived in relation to $\xi(p_1,p_2)$, wherefore these functions must satisfy the conditions of Eq. (3). Thus, $\gamma(p_1,p_2)$, and hence $\phi(p_1,p_2)$, can always be scaled by an arbitrary multiplicative constant.

2.3 Kernel of the density of states

The generalized conformal transformation introduces local changes of the density of states in the (ξ,ϕ)-space which can be expressed by means of the Jacobian

$$J(\xi,\phi) = \begin{vmatrix} \frac{\partial p_1}{\partial\xi} & \frac{\partial p_1}{\partial\phi} \\ \frac{\partial p_2}{\partial\xi} & \frac{\partial p_2}{\partial\phi} \end{vmatrix}, \tag{4}$$

which in general must be derived in the (ξ,ϕ)-space locally, in order to ensure that it is a single-valued function.

Therefore, whenever summation over quantum–mechanical states is replaced by integration over the particle's energy, one has to include also the integration over ϕ

$$\sum_{\boldsymbol{p}}\ldots = \frac{2}{(2\pi)^2}\int\mathrm{d}\xi\int\mathrm{d}\phi J(\xi,\phi)\ldots, \tag{5}$$

where the latter integral is over the whole range of ϕ. To reduce the formula to the form applied in the Van Hove scenario, we define the average density of states in the (ξ,ϕ)-space for a fixed ξ as $\nu(\xi) = \frac{2}{(2\pi)^2}\int\mathrm{d}\phi J(\xi,\phi)$, which is the usual density of states defined as $\nu(\xi) = \frac{a^2}{4\pi^2}\int\frac{\mathrm{d}f}{|\nabla_{\boldsymbol{p}}\xi_{\boldsymbol{p}}|}$.

Then, in the case when the anonymous integrand in Eq. (5) is independent of ϕ, the right-hand-side (rhs) reduces to the form postulated in the Van Hove scenario, and

$$\frac{2}{(2\pi)^2}\int\mathrm{d}\xi\int\mathrm{d}\phi J(\xi,\phi)\ldots = \int\mathrm{d}\xi\nu(\xi)\ldots.$$

However, when the integrand is a function of ξ and ϕ, as for *e.g.*, *p*- or *d*-wave paired superconductors, one must take into account that, in general,

$$\int\mathrm{d}\phi\mathcal{K}(\xi,\phi)\ldots \neq \frac{1}{\int\mathrm{d}\phi'}\int\mathrm{d}\phi'\mathcal{K}(\xi,\phi')\int\mathrm{d}\phi\ldots, \tag{6}$$

where

$$\mathcal{K}(\xi,\phi) = \frac{2}{(2\pi)^2}J(\xi,\phi)$$

is the kernel of the density of states and its value corresponds to the local deformation or modification of quantum-mechanical states in the (ξ,ϕ)-space, which is a result of the applied transformation. Moreover, the

integration of the rhs of Eq. (6) depends on the choice of ϕ. Therefore, as has been mentioned already, in some other approaches this variable is chosen as the angular variable $0 \leq \varphi < 2\pi$, identical to the one introduced in the standard polar coordinate system. Although such a choice ensures that

$$\int_0^{2\pi} \frac{\mathrm{d}\varphi}{2\pi} \mathcal{K}(\xi,\varphi)\ldots = \int_0^{2\pi} \frac{\mathrm{d}\varphi}{2\pi} \nu(\xi)\ldots, \tag{7}$$

when the anonymous integrand is independent of φ, and

$$\nu(\xi) = \int_0^{2\pi} \frac{\mathrm{d}\varphi}{2\pi} \mathcal{K}(\xi,\varphi), \tag{8}$$

it proves that the Van Hove scenario cannot be applied to other than pure s-wave pairing [7, 25].

3 Analysis of coexistence and competition between spin-singlet and spin-triplet order parameters in superconducting systems

In the present section, we illustrate the conformal transformation method by applying it to the problem of coexistence and mutual competition between the spin-singlet s- and d-waves and the spin-triplet p-wave order parameters in quasi-2D superconducting systems [9–11, 24].

As we have already mentioned, high-T_c superconducting systems, in particular copper-oxides, are regarded as quasi-2D systems with CuO_2 planes having the point group C_{4v} symmetry [8–12]. A complete analysis of such superconducting systems requires, in general, to take into account spin-fluctuation or strong-correlation effects. These can usually be incorporated into the model by means of an effective Hamiltonian of the strongly interacting Hubbard model with a given (possibly multiband) one-particle dispersion relation, which may be enriched by self-energy corrections, and a quite general form of the pairing potential $V(\boldsymbol{k},\boldsymbol{k}')$ [5, 27–31]. As we show below, the pairing interaction can be decomposed into an antisymmetric and a symmetric part, determining the spin-singlet (s- and d-wave) and spin-triplet (p-wave) symmetry of the order parameter, respectively [9–11, 24].

3.1 Statement of the problem and fundamental equations

Employing the Green function formalism, one can find two fundamental equations, consistent with the mean-field approximation. These are the gap equation in the momentum space [8–10, 24]

$$\boldsymbol{\Delta}_{\boldsymbol{k}} = \sum_{\boldsymbol{k}'} V(\boldsymbol{k},\boldsymbol{k}') \frac{\boldsymbol{\Delta}_{\boldsymbol{k}'}}{E_{\boldsymbol{k}'}} \tanh\frac{E_{\boldsymbol{k}'}}{2T}, \tag{9}$$

where $E_{\boldsymbol{k}} = \sqrt{(\xi_{\boldsymbol{k}}-\mu)^2 + \boldsymbol{\Delta}_{\boldsymbol{k}}^2}$, and another self-consistent equation

$$n = \frac{1}{N}\sum_{\boldsymbol{k}} \left(1 - \frac{\xi_{\boldsymbol{k}}-\mu}{E_{\boldsymbol{k}}} \tanh\frac{E_{\boldsymbol{k}}}{2T}\right), \tag{10}$$

which determines the total chemical potential $\mu = \mu_0 + \mu(T)$. Here, μ_0 fixes the shift of the Fermi level due to doping and is a function of the conduction band filling n, defined for the normal metallic phase at $T = 0$, whereas $\mu(T)$ expresses the temperature correction ($\mu(0) = 0$). N denotes the total number of lattice sites [9–11, 24, 32–34].

Because both the spin-singlet (s- or d-wave) symmetry states ($S = 0, M = 0$) and the spin-triplet (p-wave) symmetry state ($S = 1, M = 0$) can be formed in anisotropic superconductors, our aim is to investigate the stability of various symmetry states with regard to the properties of the system reflected in the dispersion relation. The conformal transformation method allows us also to include other factors into our study such as the carrier concentration and the particular form of the pairing potential.

In particular, we consider a 2D single-band model with a relatively wide, partially-filled conduction band of width 2ω and the dispersion relation

$$\xi_{\boldsymbol{k}} = -2t_0(\cos k_x + \cos k_y + \eta \cos k_x \cos k_y), \tag{11}$$

where $\eta = 2t_1/t_0$ and the case $\eta = 0$ corresponds to the ideal nesting. The parameters t_0, t_1 can be identified with the nearest-neighbor and the next-nearest-neighbor hopping integrals, respectively [35, 36].

Next, we need to define and analyze superconductivity with anisotropic Cooper pairing for the new quasiparticles. However, the effective interaction between quasiparticles in strongly correlated systems is quite complicated, as it in general depends on both the spin and the current carried by the quasiparticles. Because of the expected magnetically mediated pairing mechanism arising from the exchange of magnetic fluctuations, the conventional phonon-mediated pairing mechanism raises doubts. Therefore, we assume a generic, boson-mediated, strongly anisotropic attraction mechanism providing pairing interaction in the spin-antisymmetric and the spin-symmetric channels [1–3, 5, 32, 37].

Considering the Fourier-transformed generic boson-mediated potential on a square lattice, we can assume that it is translational invariant and separable, so that its matrix element $V(\boldsymbol{k},\boldsymbol{k}')$ can be rewritten as

$$V(\boldsymbol{k},\boldsymbol{k}') = V^{\mathrm{s}}(\boldsymbol{k},\boldsymbol{k}') + V^{\mathrm{a}}(\boldsymbol{k},\boldsymbol{k}'),$$

where the potentials $V^{\mathrm{s}}(\boldsymbol{k},\boldsymbol{k}') = V^{\mathrm{s}}(-\boldsymbol{k},\boldsymbol{k}') = V^{\mathrm{s}}(\boldsymbol{k},-\boldsymbol{k}')$ and $V^{\mathrm{a}}(\boldsymbol{k},\boldsymbol{k}') = -V^{\mathrm{a}}(-\boldsymbol{k},\boldsymbol{k}') = -V^{\mathrm{a}}(\boldsymbol{k},-\boldsymbol{k}')$ refer to the spin-singlet and spin-triplet pairing channels, respectively [9, 10, 24]. Moreover, these components can be presented in separable forms

$$V^{\rm s}(\boldsymbol{k},\boldsymbol{k}') = -V_0 - \sum_{j\geq 1,m} V_j^{\rm s} f_{jm}(\boldsymbol{k}) f_{jm}(\boldsymbol{k}'),$$
$$V^{\rm a}(\boldsymbol{k},\boldsymbol{k}') = -\sum_{j\geq 1,m} V_j^{\rm a} g_{jm}(\boldsymbol{k}) g_{jm}(\boldsymbol{k}'). \quad (12)$$

Then V_0 and $V_j^{\rm s,a}$ are the amplitudes in the isotropic and anisotropic channels, corresponding to the on-site term, and the nearest neighbors and the next-nearest neighbors neighbors terms, respectively. The momentum-dependent functions $f_{jm}(\boldsymbol{k}), g_{jm}(\boldsymbol{k})$, for a given j, should be taken from appropriate subsets of normalized and orthogonal basis functions of irreducible representations of the group C_{4v} defined for the 2D momentum space, including the appropriate pairing channel symmetry [9, 10, 38]. Thus, their Fermi-surface averages $\langle f_{jm}^2(\boldsymbol{k})\rangle = \langle g_{jm}^2(\boldsymbol{k})\rangle = 1$ and $\langle f_{jm}(\boldsymbol{k})\rangle = \langle g_{jm}(\boldsymbol{k})\rangle = 0$, whereas $\langle f_{im}(\boldsymbol{k}) f_{jn}(\boldsymbol{k})\rangle = \langle g_{im}(\boldsymbol{k}) g_{jn}(\boldsymbol{k})\rangle = 0$, if $i \neq j$ or $m \neq n$.

In the present paper, a boson-mediated pairing mechanism is assumed to take a phenomenological form, including isotropic on-site and anisotropic nearest-neighbor interactions on a 2D square lattice, and covering a relatively narrow region in the conduction band. In the reciprocal space, the pairing potential has the form (assuming $a_x = a_y = 1$) [5, 39–42]

$$V(\boldsymbol{k},\boldsymbol{k}') = -V_0 - V_1[\cos(k_x - k_x') + \cos(k_y - k_y')], \quad (13)$$

where the on-site potential with the amplitude V_0 can be either repulsive or attractive, whereas the nearest neighbor potential (amplitude V_1) is always attractive. Both vanish beyond the cut-off energy $\pm\omega_{\rm c}$. After some algebraic computaions, the potential (13) can be transformed into the following separated forms [5, 8–10, 24, 39]

$$V^{\rm s}(\boldsymbol{k},\boldsymbol{k}') = -V_0 - \frac{1}{2}V_1(\cos k_x + \cos k_y)(\cos k_x' + \cos k_y') - \frac{1}{2}V_1(\cos k_x - \cos k_y)(\cos k_x' - \cos k_y'), \quad (14)$$
$$V^{\rm a}(\boldsymbol{k},\boldsymbol{k}') = -V_1(\sin k_x \sin k_x' + \sin k_y \sin k_y') \quad (15)$$

compatible with irreducible representations of the group C_{4v} in the 2D momentum space, and consistent with (12).

Hence, in order to take into account both the form of the dispersion relation (11) and that of the pairing potential (14) and (15), for the 2D momentum space, the subsets of the basis functions of the irreducible representations of the group C_{4v} are usually taken in the following simplest forms (*cf.* Appendix B):

$$\{\cos k_x + \cos k_y\}, \quad (16)$$
$$\{\cos k_x - \cos k_y\}, \quad (17)$$
$$\{\sin k_x \sin k_y\}, \quad (18)$$
$$\{\sin k_x \sin k_y(\cos k_x - \cos k_y)\} \quad (19)$$
$$\{\sin k_x, \sin k_y\}. \quad (20)$$

Since the function of the first subset (16) corresponds to the trivial irreducible representation, this set is sometimes replaced equivalently by $\{1\}$. A complete, group-theoretical discussion of the symmetry properties of the invariant sets is given in Appendix B.

We emphasize that the above choice is one of many possibilities and that these functions can be replaced by some more composed forms. In particular, multiplying them by $(1 - \cos k_x \cos k_y)^{-1}$ results in setting up another set of functions being invariants of the group C_{4v} [32]. Moreover, the subset of basis functions corresponding to the irreducible representations can be taken, e.g., as

$$\{\cos k_x + \cos k_y + \eta_1 \cos k_x \cos k_y\}, \quad (21)$$
$$\{(\cos k_x - \cos k_y)[1 + \eta_2(\cos k_x + \cos k_y)]\}, \quad (22)$$
$$\{\sin k_x \sin k_y[1 + \eta_3(\cos k_x + \cos k_y)]\}, \quad (23)$$
$$\{\sin k_x \sin k_y(\cos k_x - \cos k_y)[1 + \eta_4(\cos k_x + \cos k_y)]\}, \quad (24)$$
$$\{\sin k_x[1 + \eta_5(\cos k_x + \cos k_y)], \sin k_y[1 + \eta_5(\cos k_x + \cos k_y)]\}, \quad (25)$$

where $\eta_1, \eta_2, \ldots, \eta_5$ are real numbers.

The functions of Eqs. (16)–(18), which are invariants of the group C_{4v}, are usually applied to represent the pairing interaction, Eqs. (14) and (15). Similarly, the dispersion relation, Eq. (11), can be expressed by means of the function of Eq. (21), which is another invariant of the group C_{4v}, fixed for the trivial irreducible representation. Although the symmetry properties of the functions in Eqs. (16) and (21) defined by elements of the group C_{4v} are identical, these functions are not equivalent, except for the case $\eta_l = 0$. This means that if $\eta_l \neq 0$, two different sets of basis functions appear.

3.2 Conformal transformation and the structure of the pairing-potential

In the next step we employ the conformal transformation method [9–11, 24–26, 32], which allows us to rewrite the two fundamental Eqs. (9) and (10) in the new coordinate system (ξ, φ), where ξ stands for the one-particle energy and φ is the angular variable of the standard polar coordinate system. Let us emphasize again that the formalism can be regarded as an extended Van Hove scenario [24, 25] valid for superconducting systems with anisotropic pairing, maintaining the correct number of degrees of freedom in a 2D reciprocal space. As we emphasized earlier, this transformation introduces the Jacobian of what can be treated as the kernel of the density of states corresponding to the local deforma-

tion or modification of quantum-mechanical states in the (ξ,φ)–space.

The coordinates k_x, k_y and the kernel of the density of states as functions of ξ,φ, for the tight-binding model with the particle-hole asymmetry parameter η, are found as [9–11, 24–26, 32]

$$k_x(\xi,\varphi,\eta)=\arccos\frac{1}{\eta}[X(\xi,\varphi,\eta)-1],$$
$$k_y(\xi,\varphi,\eta)=\arccos\frac{1}{\eta}[Y(\xi,\varphi,\eta)-1], \tag{26}$$

and

$$\mathcal{K}(\xi,\varphi,\eta)=\frac{\eta^2}{4\pi t_0}\frac{1}{\sqrt{\eta^2-[X(\xi,\varphi)-1]^2}\sqrt{\eta^2-[Y(\xi,\varphi)-1]^2}}\times\frac{1}{[X(\xi,\varphi)]^2+[Y(\xi,\varphi)]^2}\frac{1}{1+\sin 2\varphi}\phi_0(\xi), \tag{27}$$

where

$$X(\xi,\varphi,\eta)=\left[\sqrt{\left(1-\eta\frac{\xi}{2t_0}\right)^2+\eta^2\phi_0^2(\xi)f^2(\varphi)}+\eta\phi_0(\xi)f(\varphi)\right]^{\frac{1}{2}},$$

and

$$Y(\xi,\varphi,\eta)=\left[\sqrt{\left(1-\eta\frac{\xi}{2t_0}\right)^2+\eta^2\phi_0^2(\xi)f^2(\varphi)}-\eta\phi_0(\xi)f(\varphi)\right]^{\frac{1}{2}},$$

whereas

$$\phi_0(\xi,\eta)=\begin{cases}\dfrac{1}{2(1+\eta)^2}\left|2+\eta+\dfrac{\xi}{2t_0}\right|\left|2+2\eta+\eta^2-\eta\dfrac{\xi}{2t_0}\right|, & \text{if}\quad \dfrac{\xi}{2t_0}\le\eta\\ \dfrac{1}{2(1-\eta)^2}\left|2-\eta-\dfrac{\xi}{2t_0}\right|\left|2-2\eta+\eta^2-\eta\dfrac{\xi}{2t_0}\right|, & \text{if}\quad \dfrac{\xi}{2t_0}\ge\eta\end{cases}$$

and

$$f(\varphi)=\frac{\sin\varphi-\cos\varphi}{\sin\varphi+\cos\varphi}. \tag{28}$$

Note that $\phi_0(\xi,\eta)=\phi_0(-\xi,-\eta)$, $X(\xi,\varphi,\eta)=Y(-\xi,\varphi,-\eta)$, and $\mathcal{K}(\xi,\varphi,\eta)=\mathcal{K}(-\xi,\varphi,-\eta)$. The density of states can then be defined by [9–11, 24–26, 32]

$$\nu(\xi,\eta)=\frac{2}{\pi}\int_0^{\pi/2}\mathrm{d}\varphi\mathcal{K}(\xi,\varphi,\eta), \tag{29}$$

and $\nu(\xi,-\eta)=\nu(-\xi,\eta)$.

Consequently, the functions describing the spin-singlet and spin-triplet pairing channels can be expanded in a double Fourier series in the angular variable. Because the spatial structure of the order parameter is determined by the dominating coefficient of the Fourier expansion, the symmetry of the order parameter can be identified with respect to the harmonic functions $\sin n\varphi$ and $\cos n\varphi$ [8–10, 24, 25, 39, 43]. In the case when one Fourier component dominates the others, the form of the symmetric (14) and antisymmetric (15) components of the pairing potential, responsible for the formation of the spin-singlet (s- and d-wave) and spin-triplet (p-wave) order parameters, respectively, read

i) Pure s-wave pairing

$$V^{\mathrm{s}}(\xi,\varphi;\xi',\varphi')=-V_0-U_0(\eta,n)v_0(\xi,\eta,n)v_0(\xi',\eta,n).$$

ii) Pure p-wave pairing

$$V^{\mathrm{a}}(\xi,\varphi;\xi',\varphi')=-2U_1(\eta,n)v_1(\xi,\eta,n)v_1(\xi',\eta,n)\times[\cos\varphi\cos\varphi'+\sin\varphi\sin\varphi'].$$

iii) Pure d-wave pairing

$$V^{\mathrm{s}}(\xi,\varphi;\xi',\varphi')=-2U_2(\eta,n)v_2(\xi,\eta,n)\times v_2(\xi',\eta,n)\cos 2\varphi\cos 2\varphi'.$$

Here, for $l=0,1$, or 2, $v_l(\xi,\eta,n)=\chi_l(\xi,\eta)/\bar{\chi}_l(\eta,n)$, the carrier concentration $n=n(\eta,\mu_0)$ and

$$\bar{\chi}_l(\eta,n)=\frac{1}{2\omega_{\mathrm{c}}}\int_{-\omega_{\mathrm{c}}+\mu_0}^{\omega_{\mathrm{c}}+\mu_0}\chi_l(\xi,\eta)\mathrm{d}\xi$$

is the (η,n)-dependent mean value of the Fourier coefficient $\chi_l(\xi,\eta)$ in the pairing region of width $2\omega_{\mathrm{c}}$. Group-theoretical symmetry properties of the separable parts of the pairing potential in the new (ξ,φ) space are discussed in Appendix C.

The function $U_l(\eta,n)=V_1[\bar{\chi}_l(\eta,n)]^2$ defines the modified coupling coefficient for a particular pairing channel, satisfying the symmetry relation $U_l(\eta,n(\eta,\mu_0))=U_l(-\eta,n(-\eta,-\mu_0))$ for $l=0,1$ and $l=2$. Because the purely s-wave pairing potential is also modified (enhanced or diminished) by the constant term V_0 corre-

sponding to the on-site interaction, the s-wave symmetry superconducting state may prevail for sufficiently large and positive V_0 or it may be completely eliminated from the system for sufficiently large and attractive V_0.

Note that the separable forms 1–3 of the reduced pairing potential imply the following symmetry of the order parameter: $\mathbf{\Delta}(\xi,\varphi,l,\eta,n)=\Delta(T)v_l(\xi,\eta,n)D(\varphi,l)$, with

$$D(\varphi,0)=1, \quad \text{for } s\text{-wave pairing},$$
$$D(\varphi,1)=\sqrt{2}\cos(\varphi+\beta_1), \quad \text{for } p\text{-wave pairing},$$
$$D(\varphi,2)=\sqrt{2}\cos 2\varphi, \quad \text{for } d\text{-wave pairing},$$

and only $\beta_1=0,\pm\pi/4,\pi/2$ should be included [9].

With regard to the Fourier-transformed generic boson-mediated potentials, the presented method of expanding the pairing potential in a double series of Fourier harmonics ($\sin n\varphi$ and $\cos n\varphi$) is more effective than that previously discussed, since the coefficients of the Fourier expansion define pairing amplitudes of a definite symmetry. Consequently, in the case of magnetically mediated superconductivity [1–3], where spin-fluctuation modes contribute to the pairing amplitudes in the singlet and triplet channels in a different manner, the p-wave spin-triplet pairing appears in nearly ferromagnetic metals. On the other hand, the d-wave spin-singlet pairing appears in nearly antiferromagnetic metals, which corresponds to opposite values of the fixed parameter (± 2). Thus, one can suspect that the p- and d-wave pairing amplitudes exchange their domination regimes when this fixed parameter takes the opposite value.

In a general situation, the form of the interaction in the pairing channel not only affects the symmetry of the energy gap, but may also induce some additional effects, e.g., opening of the gap above the critical temperature (pseudogap behavior). This kind of effects can also be modeled within the conformal transformation method. In particular, the conformal transformation method has been successfully applied in the description of a singular Fermi liquid system with a discriminating interaction in spin space, which prevents double-occupation of states with a given momentum [44, 45]. In that system, a non-zero solution of the superconducting gap equation above the critical temperature was found and attributed to pseudogap behavior. Recently, other mechanisms in the pairing channel, which result in the appearance of the pseudogap in underdoped cuprates, have also been suggested and discussed [46].

3.3 Phase diagrams for stable superconducting states

According to the experimental data [28, 35, 47–57], the dimensionless parameter η in the 2D single-band tight-binding dispersion relation for cuprate materials is negative and $|\eta|\leq 0.9$. On the other hand, its value assessed within the 2D t–J model with an antiferromagnetic background, employing the quantum Monte Carlo method, is positive and can take values up to 1.53. Taking $t_0=0.24$ eV or 0.35 eV [35], ω_c ranging from 26 meV to 65 meV [28], and including the results of the local density approximation band structure calculations, where the band structure of YBCO was considered in the $\epsilon_F\pm 2$ eV range [30, 31], we may choose $\omega_c/(2t_0)\approx 0.1$ and $\omega/\omega_c=11$ for numerical evaluations. We also take into account that $-0.9\leq\eta\leq 0.9$, and demand that the effective dimensionless pairing coefficient satisfies the weak-coupling condition: $\frac{1}{2}\nu_0(\eta)U_2(\eta)<0.41$. In the present study, we focus on the cases when $V_1/2\pi t_0=0.6,1$, or 1.9 and the ratio $\upsilon=V_0/V_1$ ranges from -0.61 to 0.90. This allows us to study some superconducting systems with a partially filled conduction band, when the chemical potential $-1\leq\mu_0/(2t_0)\leq 1$. Then, the carrier concentration n varies between the lower limit of 0.02 to 0.14 and the upper limit of 0.98 to 0.86.

The transformed equations (9) and (10) can be used to derive the order parameter amplitude $\Delta(T)$ and the chemical potential $\mu=\mu_0+\mu(T)$ of the superconducting phase with the symmetry corresponding to $l=0,1$, or 2, for fixed carrier concentration n. In the limit $T=T_c$ these equations can be written in the following reduced forms [9–11, 24]

$$1=[V_0\,\delta_{0,l}+U_l(\eta,n)]\int_0^{2\pi}\frac{\mathrm{d}\varphi}{2\pi}\int_{-\omega_c}^{\omega_c}\mathrm{d}\xi\mathcal{K}(\xi+\mu_0,\varphi,\eta)\times\frac{D^2(\varphi,l)}{\xi-\mu(T_c)}\tanh\frac{\xi-\mu(T_c)}{2T_c}, \tag{30}$$

where we assume that $v_l(\xi+\mu_0,\eta)\cong 1$. Consequently, Eq. (10) reads

$$n=\frac{1}{N}\int_0^{2\pi}\frac{\mathrm{d}\varphi}{2\pi}\int_{-\omega_c}^{\omega_c}\mathrm{d}\xi\,\mathcal{K}(\xi,\varphi,\eta)\times\left[1-\tanh\frac{\xi-\mu_0-\mu(T_c)}{2T_c}\right]. \tag{31}$$

Examining Eq. (10) in the limit $T=0$, the carrier concentration n can be found as a function of η and μ_0 for a fixed bandwidth 2ω. This relation is presented in Fig. 1. Note that the relation implies that $n(-\eta,\mu_0)=1-n(\eta,-\mu_0)$ [9, 10, 24].

Our next goal is to determine the stability regions for s-, p-, and d-wave symmetry superconducting states in the (η,n)–plane for selected values of the ratio $\upsilon=V_0/V_1$ and a fixed amplitude V_1. These stability regions, which nucleate during the phase transition from the normal to superconducting phase, can be found by comparing the transition temperatures $T_c(l,\eta,n)$, found self-consistently from Eqs. (30) and (31), for fixed values of l, η, and μ_0. According to the established relations [8–10, 24, 25, 43] the transition temperatures satisfy the relation $T_c(l,-\eta,n(-\eta,\mu_0))=T_c(l,\eta,n(\eta,-\mu_0))$ for

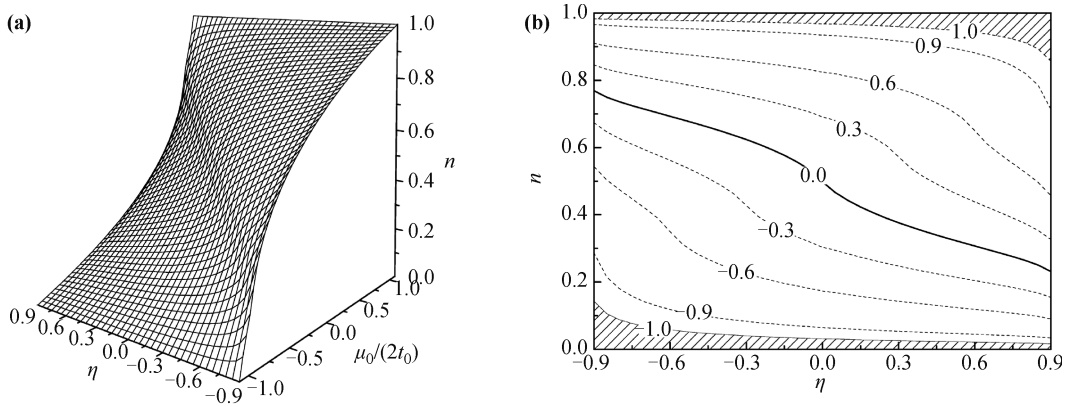

Fig. 1 The carrier concentration n as a function of $\eta = 2t_1/t_0$ and μ_0 for the band width $2\omega = 4.4t_0$: **(a)** 3D plot and **(b)** equi-concentration lines for $\mu_0/(2t_0) = 0, \pm 0.3, \pm 0.6, \pm 0.9, \pm 1.0$. In this and the following figures, the region permitted for the variables η and n, resulting from their relation to μ_0, is shown as the unshaded area.

$l = 0, 1, 2$.

3.3.1 BCS–type approximation

Before we move on to discuss the results of the tight-binding model, we also employ a BCS-type approximation to provide a reference point. Within this approximation, the kernel of the density of states $\mathcal{K}(\xi, \varphi, \eta)$ is replaced by the average value of the usual density of states, i.e.,

$$\nu_0(\eta) = \frac{1}{2\omega} \int_{-\omega_c}^{\omega_c} \mathrm{d}\xi \nu(\xi, \eta), \tag{32}$$

and the transition temperature can be found from the formula

$$T_{c0}(l, \eta, n) = \frac{2e^{\gamma}}{\pi} \omega_c \exp\left\{ -\frac{2}{\nu_0(\eta)[V_0\, \delta_{0,l} + U_l(\eta, n)]} \right\}, \tag{33}$$

where $\gamma \approx 0.577$ is the Euler constant, or $T_{c0}(l, \eta, n) = 0$ if $V_0\, \delta_{0,l} + U_l(\eta, n) \leq 0$. Moreover, we have $T_{c0}(l, -\eta, n(-\eta, \mu_0)) = T_{c0}(l, \eta, n(\eta, -\mu_0))$ for $l = 0, 1, 2$.

A general observation can be formulated based on the results of the BCS-type approximation (cf. Fig. 2). We see that the s-wave state is preferred for a low concentration if $\eta < -0.4$ and for a high concentration if $\eta > -0.4$. In addition, the d-wave state should be realized for sufficiently large $|\eta|$ (negative as well as positive) and moderate n, and in the other parts of the diagram the p-wave state prevails. On the other hand, close to the boundary between the regions with a definite symmetry of the order parameter, one can find states where the spin-singlet s-wave and spin-triplet p-wave, the spin-singlet d-wave and spin-triplet p-wave, or the spin-singlet s-wave and spin-singlet d-wave order parameters coexist. Such *triple points* can be clearly identified in the phase diagrams (Table 1).

Detailed calculations within the BCS-type approximation illustrate how the stability areas of the s-wave order parameter gradually fill up the diagram with increasingly attractive on-site interaction ($V_0 > 0$), and how they are being eliminated when this interaction becomes repulsive ($V_0 < 0$). The diagrams of stable superconducting states obtained for $\upsilon = V_0/V_1 = -0.25, 0.25, 0.5$ and 0.6 are presented in Fig. 2. Moreover, the s-wave order parameter is stable in the whole diagram area only if $\upsilon \geq 0.64$. On the other hand, for $\upsilon \leq -0.61$, it is completely repelled from the diagram ($-0.9 \leq \eta \leq 0.9$ and $0 \leq n \leq 1$). Hence, the triple points of coexistence of s-, p-, and d-wave order parameters emerge in the diagrams for positive and negative values of V_0 from a certain range, although their location changes.

Table 1 Positions of the triple points in the diagrams of Fig. 2 found within the BCS-type approach for various values of the ratio υ.

υ	-0.25	0	0.25	0.5
(η, n)	$(-0.87, 0.17)$	$(-0.79, 0.18)$	$(-0.67, 0.24)$	$(-0.43, 0.42)$
(η, n)	$(0.87, 0.83)$	$(0.79, 0.82)$	$(0.67, 0.76)$	$(0.43, 0.58)$

3.3.2 Single-band tight-binding model

Based on the results obtained in the BCS-type approximation, we may expect that stable areas of the s-wave order parameter will become larger for $V_0 > 0$ and shrink for $V_0 < 0$ also in the tight-binding approach. To verify this claim and make more precise observations for the single-band tight-binding model, we plot the corresponding phase diagrams also in this case. The diagrams in Figs. 4 and 5 illustrate the result obtained for three values of the pairing amplitude $V_1/(2\pi t_0) = 0.6, 1$, or 1.9 after replacing μ_0 with n and a mutual comparison of the transition temperatures $T_c(0, \eta, n)$, $T_c(1, \eta, n)$,

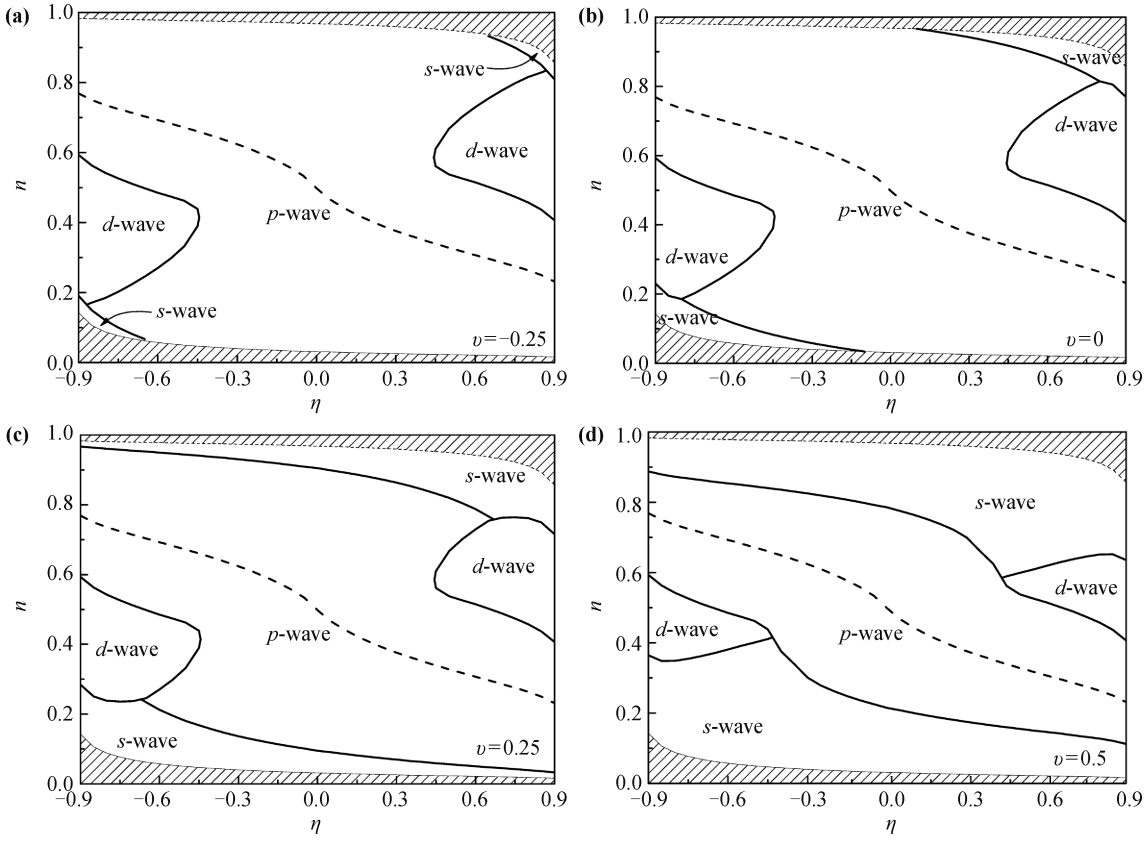

Fig. 2 Phase diagrams of the stable spin-singlet s- and d-wave, and spin-triplet p-wave superconducting states found within the BCS-type approximation. The diagrams evolve significantly with changes in the ratio $\upsilon = V_0/V_1$: **(a)** $\upsilon = -0.25$, **(b)** $\upsilon = 0$, **(c)** $\upsilon = 0.25$, and **(d)** $\upsilon = 0.5$.

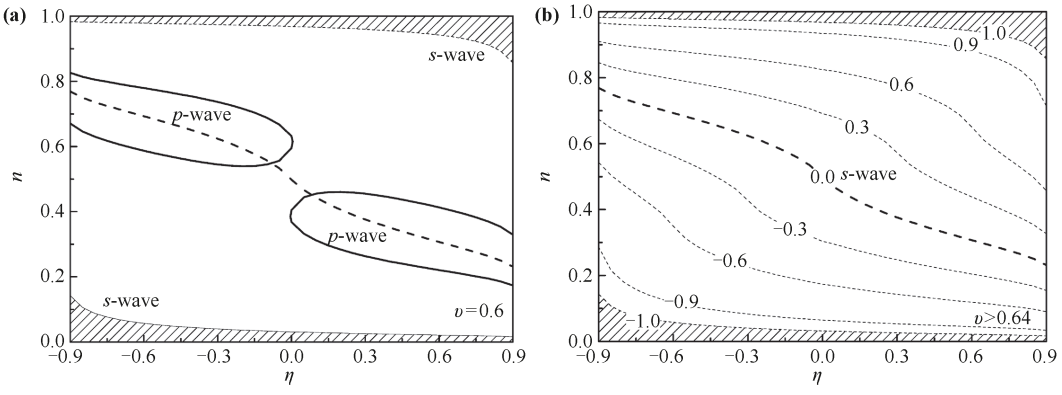

Fig. 3 **(a)** Expulsion of the spin-singlet d-wave state from the diagram obtained within the BCS-type approximation for $\upsilon = 0.6$. **(b)** Further increase in the value of the ratio υ beyond 0.64 leads to complete expulsion of the spin-triplet p-wave state, leaving the s-wave symmetry state as the only stable superconducting state.

and $T_c(2, \eta, n)$, when the values of the $\upsilon = V_0/V_1$ ratio are equal to $-0.25, 0, 0.25, 0.5, 0.6, 0.7, 0.85$, and 0.9. We emphasize that within the discussed model, the boundary condition $T_c(0, \eta, n) = T_c(1, \eta, n)$ coincides with the relation $T_{c0}(0, \eta, n) = T_{c0}(1, \eta, n)$ for all values of υ [9, 10, 24, 25].

In Fig. 4, we present diagrams of the stability areas with the s-, d-, and p-wave order parameters revealed. They appear for $-0.9 \leq \eta \leq 0.9$ and $n_d < n < n_u$, where $n_d = n(\eta, \mu_0/(2t_0) = -1) > 0$ and $n_u = n(\eta, \mu_0/(2t_0) = 1) < 1$. The stability areas for the order parameters of various symmetries can be observed

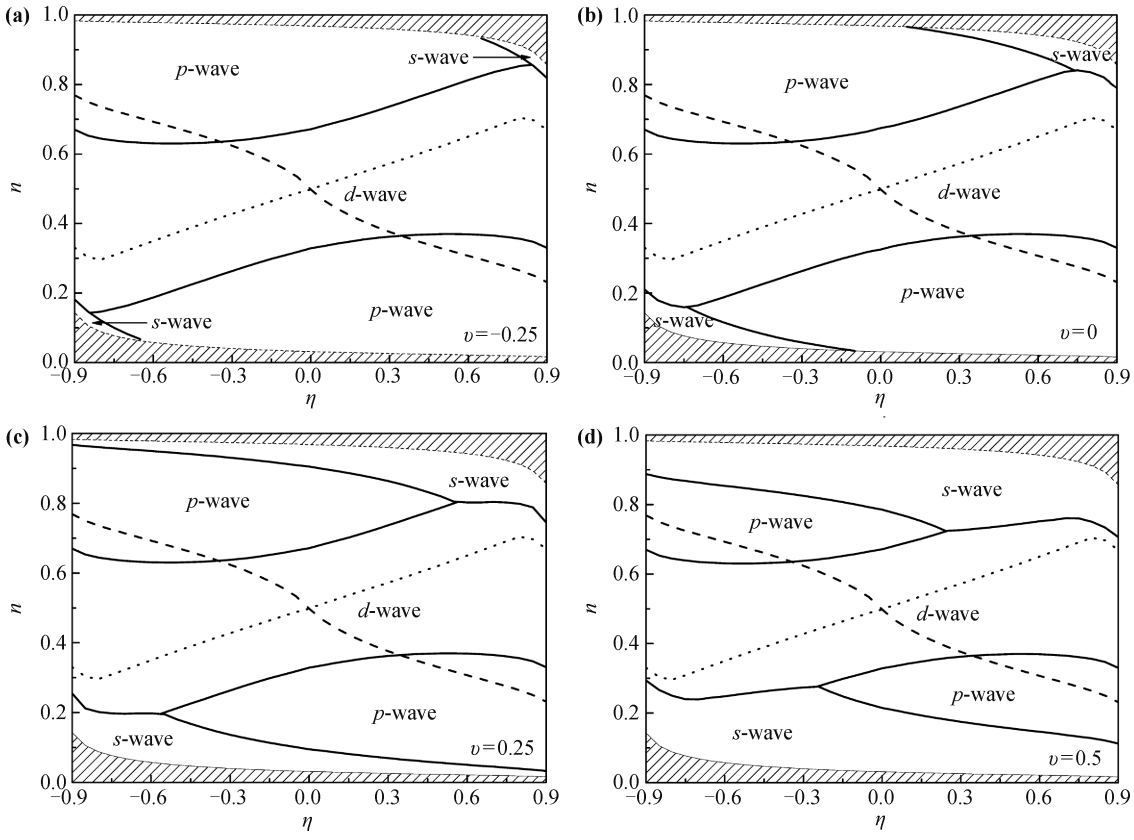

Fig. 4 Phase diagrams of stable spin-singlet s- and d-wave, and spin-triplet p-wave superconducting states found within the single-band tight-binding model. The diagrams clearly evolve with the change of the ratio $\upsilon = V_0/V_1$: **(a)** $\upsilon = -0.25$, **(b)** $\upsilon = 0$, **(c)** $\upsilon = 0.25$, and **(d)** $\upsilon = 0.5$. The supreme values of the transition temperature within the d-wave state stability area are attained along the dotted line. The half-filled conduction band $[\mu_0/(2t_0) = 0]$ is denoted by the dashed line. The triple-point positions are given in Table 2.

in the presented diagrams when $-0.61 < \upsilon < 0.64$. In particular, the s-wave state emerges in the diagram if $\upsilon \geq -0.61$, and is preferred for low and high concentration n if υ is negative, zero, or positive (although small). The stability areas for the s-wave state expand when υ increases [Fig. 4 and Figs. 5(a–c)], so that the p-wave state is eventually eliminated from the diagram for $\upsilon \geq 0.64$ [Figs. 5(b–d)]. The diminishing area of the stable d-wave state forms an island in the s-wave order parameter sea [Fig. 5(c)], and occupies the central part of the diagram for υ up to approximately 0.9. For larger values of υ, only the s-wave state can be realized in the system.

Note that the stability areas for the s-wave, d-wave, and p-wave order parameters have been evaluated in the limit $\Delta(T) \to 0$. Therefore, pure-symmetry states exist in these areas only, which are separated from the others by phase-transition lines. However, one can expect that, in the superconducting phase, when the temperature T is very close to $T_c(l, \eta, n)$, the phase transition lines broaden proportionally to $(T_c(l, \eta, n) - T)$. Then one can find regions—near to the boundaries between the distinguished areas—where the spin-singlet s- and spin-triplet p-wave, the spin-singlet d- and spin-triplet p-wave, or the spin-singlet s- and spin-singlet d-wave order parameters coexist [Fig. 4 and Figs. 5(a–c)].

Similar to the BCS-type approximation, also in the tight-binding model diagrams there appear triple points around which the spin-singlet s-wave and d-wave, and spin-triplet p-wave order parameters can coexist [Fig. 4 and Fig. 5(a)]. The estimated locations of the triple points are given in Table 2. The supreme values for the transition temperature found for a given value of the parameter η are located along the dotted line in the d-wave order parameter region in Figs. 4 and 5. Note that the dotted line always goes through the central point of the diagrams $(\eta = 0, n = 0)$, and that the highest transition temperatures are attained for the d-wave superconducting state.

In Fig. 5, we can clearly see shrinking stability areas for the d-wave and p-wave order parameters, which are eventually eliminated from the diagrams by the s-wave order parameter. The stability areas for the p-wave order parameter can be found in the diagram if $\upsilon < 0.64$, whereas the stability areas for the d-wave order parameter survive until $\upsilon = 0.9$.

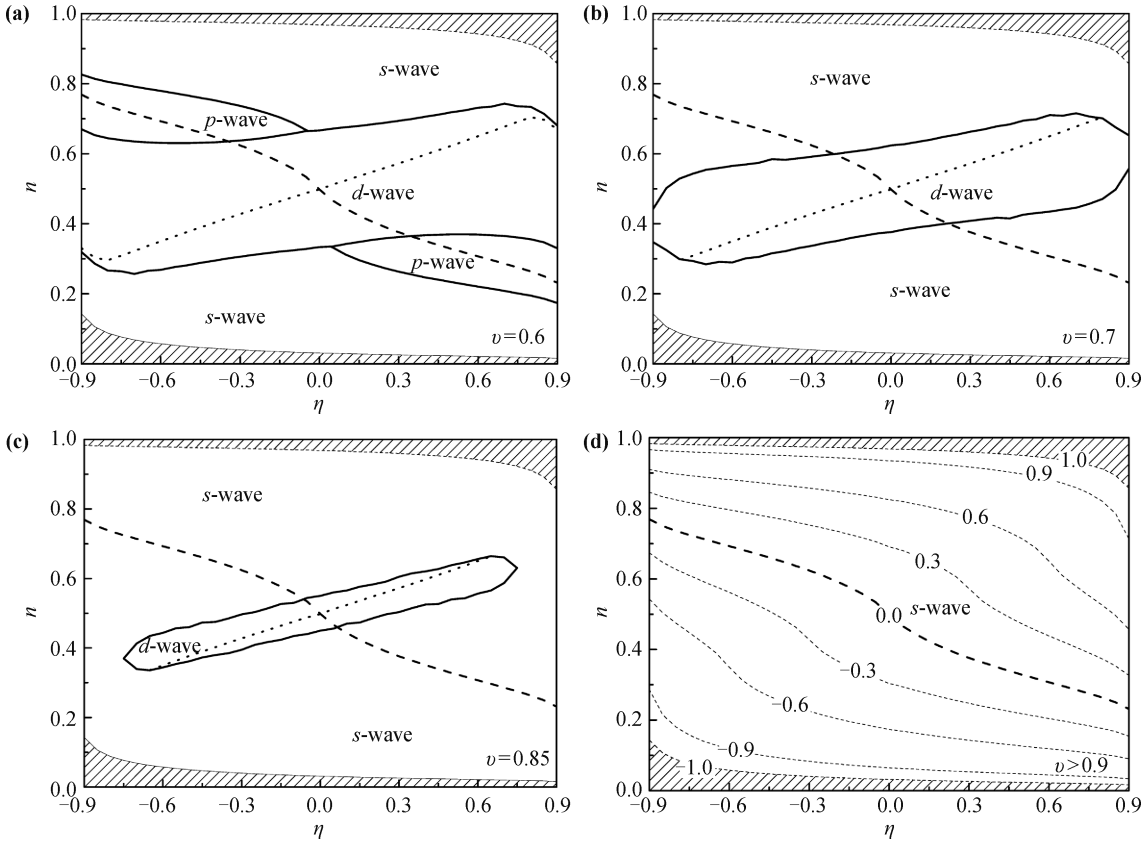

Fig. 5 Expulsion of the stable spin-singlet d- and spin-triplet p-wave superconducting states from the diagrams by the spin-singlet s-wave superconducting state. The results are obtained within the single-band tight-binding approach for various values of the $\upsilon = V_0/V_1$ ratio. **(a)** The stability areas of the three discussed states for $\upsilon = 0.6$ survive until $\upsilon < 0.64$. **(b)** The p-wave state has been eliminated ($\upsilon = 0.7$). **(c)** The d-wave state for $\upsilon = 0.85$ forms an island around the central point ($\eta = 0, n = 0$) of the diagram. **(d)** Only the s-wave state can be realized in the system for $\upsilon \geq 0.9$. In panels (a)–(c) the supreme values of the transition temperature within the d-wave state stability areas are attained along the dotted line. The half-filled band concentration [$\mu_0/(2t_0) = 0$] is denoted by the dashed line. In panel (d) the equi-concentration lines for $\mu_0/(2t_0) = \pm 0.3, \pm 0.6, \pm 0.9$, and ± 1.0 are shown as thin dashed lines.

Table 2 Positions of the triple-point positions in the diagrams in Fig. 4 and Fig. 5(a) found within the tight-binding approach for various values of the $\upsilon = V_0/V_1$ ratio.

υ	-0.25	0	0.25	0.5	0.6
(η, n)	$(-0.84, 0.14)$	$(-0.75, 0.16)$	$(-0.56, 0.20)$	$(-0.24, 0.28)$	$(0.046, 0.33)$
(η, n)	$(0.84, 0.86)$	$(0.75, 0.84)$	$(0.56, 0.80)$	$(0.24, 0.72)$	$(-0.046, 0.67)$

In the case of the 2D tight-binding band model, the conformal transformation method allowed us to have both the dispersion relation and the structure of the pairing potential included in the discussion [8–10]. The results obtained show that in the case of a nearly half-filled conduction band, the spin-singlet d-wave symmetry superconducting state remains stable for small values of the parameter η, even if a strong attractive on-site interaction is present (Figs. 4 and 5). Hence, the d-wave state should be able to compete with the s-wave state in some doped systems. It is worth to compare this conclusion with the results obtained within the BCS-type approximation by employing Eq. (33); the BCS-type calculation reveals strong domination of the s-wave state in the presence of an attractive on-site interaction (Fig. 3). The s-wave order parameter is stable in the whole diagram if $\upsilon \geq 0.64$ (see Fig. 3), and it is completely eliminated from the diagram if $\upsilon \leq -0.61$ [10, 24]. The boundaries established between the stability areas of the s- and p-wave order parameters partially coincide with some of those obtained for the tight-binding model, while the boundaries between the stability areas for the p- and d-wave order parameters keep their shape. This results in a shift of the triple points.

Since the transition temperatures depend on η, n, υ, and the order parameter symmetry, they vary essentially within the diagrams and amongst themselves. This allows us to argue that in some high-T_c superconductors

of similar molecular composition, different symmetry order parameters can nucleate during the phase transition. Moreover, an isotropic on-site interaction and contributing anisotropic nearest-neighbor interactions can significantly modify the stability regions in the diagrams.

Although the above discussion involves the case $\Delta(T) \to 0$ and can refer only to temperatures very close to $T_c(l,\eta,n)$, which are the ones most intensively investigated in the experiment, the developed formalism can also be employed to study the stability of the order parameters for temperatures from 0 to $T_c(l,\eta,n)$. Note that, for states with specified symmetry of the order parameter and fixed n, the energy gap $\Delta(T)$ as well as $\mu = \mu_0 + \mu(T)$ can both be derived from the transformed equations (9) and (10) independently [9]. Then, the free energy difference can be found by employing some universal relations between the energy gap $\Delta(T)$ and the thermodynamic potential difference defined between the superconducting and the normal phase [59], and the chemical potential of the superconducting phase. After comparison of the free energy differences for the given model parameters and temperature, one can identify the stable order parameter. The whole procedure, however, is quite tedious.

4 Conclusions

Within the presented conformal transformation method, an anisotropic crystal, with an established one-particle (quasi-particle) dispersion relation, can be considered an isotropic Fermi liquid with an imposed scalar field of the density of states. This field includes all the symmetry properties of the system, and can be introduced into the BCS–type theory along with any pairing interaction. This makes the method particularly suitable for studies of high T_c superconductors. It is also worth to emphasize that the symmetry features of s–paired superconductors are included only in a residual form, averaged over equi-energy surfaces (lines). These general characteristics of the superconducting state imply that most of the low T_c superconductors reveal similar properties, which is the reason for the great success of the BCS theory. On the other hand, in the case of high T_c new generation materials, the different thermodynamic properties and the enhancement of the critical temperature observed in the experiment, result from a great number of Van Hove singularities on the equi-energy surfaces (lines). These singularities may significantly modify the density of states in the vicinity of the Fermi level. Moreover, modification of the stoichiometric structure of a superconductor may change the shape of its equi-energy surfaces (lines) and thereby some Van Hove singularities may compensate for others. As a consequence, some fluctuations in the density of states vanish, and the superconductor may lose its extraordinary properties.

To illustrate the versatility of the proposed method, we have applied it to study effects implied by the features of the pairing potential and dispersion relation. Comparing the results of the tight-binding approach and those obtained for the simplified BCS-type approximation one should note the fundamental differences in the topology of the phase diagram with regard to the stability areas of the s-, p-, and d-wave order parameters, and their gradual evolution. The results prove that the ratio of the pairing amplitudes $\upsilon = V_0/V_1$ and that of the hopping parameters $\eta = 2t_1/t_0$, as well as the carrier concentration n, significantly influence the transition temperature. Numerical calculations within the tight-binding band model reveal that the spin-singlet d- or s-wave, and the spin-triplet p-wave symmetry superconducting states can be stable in large areas of the (η, n) plane for all values of η (*i.e.*, $|\eta| \leq 0.9$), if one fixes the carrier concentration n properly. The regions near the boundary between the areas of stable states seem to be of special interest, because two different order parameters may coexist there. The observation of coexistence of the s-, d-, and p-wave order parameters around triple points in the diagrams could be possible for various doped samples if $-0.61 \leq \upsilon \leq 0.64$ [9, 10, 24, 28, 58]. Beyond these limits, the triple points are eliminated from the diagrams and, eventually, the s-wave order parameter is being strongly suppressed or fully favored.

Note that although the parameter η is fixed and constant for each superconducting sample, one can modify η by placing it in a uniform perpendicular magnetic field. Since we take into account the spin-triplet paired states with the spin projection $S_z = 0$ and the spin-singlet paired states, which are affected by the magnetic field due to the Zeeman coupling, which, being ineffective, leads only to the renormalization of the chemical potential $\mu \mapsto \bar{\mu} = \mu \pm \frac{1}{2} g \mu_B H$. Therefore, the role of the magnetic field H is to move singularities in the kernel of the density of states $\mathcal{K}(\xi, \varphi)$, and in the density of states itself, away from the Fermi surface, and to reduce the enhancement of the transition temperature [60]. Therefore, for sufficiently large H the field-induced transition from the spin-singlet to the spin-triplet superconductivity should eventually be observed. Indeed, this has been reported recently [33].

Acknowledgements This work was supported by the Polish Ministry of Science and Higher Education (MNiSW) in 2015/2016.

Appendix A: Curvilinear transformations

General properties of curvilinear transformations and their relation to the density of states and its kernel can be considered as follows: For two arbitrary, orthogonal, curvilinear coordinate systems in a d-dimensional space, $x_1, \ldots, x_d$ and $y_1, \ldots, y_d$, where $d = 2$ or 3, the

coordinates of a vector in the former system can always be expressed as functions of coordinates in the latter one, i.e., $x_i = x_i(y_1, \ldots, y_d)$ and $y_j = y_j(x_1, \ldots, x_d)$, where $i, j = 1, \ldots, d$, and $\hat{\boldsymbol{x}}_1, \ldots, \hat{\boldsymbol{x}}_d$ is a basis of orthogonal unit vectors associated with the point $[x_1, \ldots, x_d]$ of this space. Since we consider curvilinear systems, their basis vectors defined for particular points of the space can be randomly oriented. The infinitesimal translation vector fixed at the point $[x_1, \ldots, x_d]$ has the form $\mathrm{d}\boldsymbol{x} = \sum_{i=1}^{d} \hat{\boldsymbol{x}}_i \mathrm{d}x_i$, whereas the same vector $\mathrm{d}\boldsymbol{x}$ in the other coordinate system can be expressed as $\mathrm{d}\boldsymbol{x} = \sum_{i=1}^{d} \frac{\partial \boldsymbol{x}}{\partial y_i} \mathrm{d}y_i$, where the vectors $\hat{\boldsymbol{y}}_i = \frac{\partial \boldsymbol{x}/\partial y_i}{|\partial \boldsymbol{x}/\partial y_i|}$ form an orthonormal basis of the other coordinate system. They are tangent to the lines y_i, so for particular points of the space they are randomly oriented as well. The relation

$$\mathrm{d}y_i = \nabla_{\boldsymbol{x}} y_i \cdot \mathrm{d}\boldsymbol{x} = \sum_{j=1}^{d} \nabla_{\boldsymbol{x}} y_i \cdot \frac{\partial \boldsymbol{x}}{\partial y_j} \mathrm{d}y_j,$$

fulfilled for each coordinate y_i, implies that

$$\nabla_{\boldsymbol{x}} y_i \cdot \frac{\partial \boldsymbol{x}}{\partial y_j} = \delta_{ij}. \tag{A1}$$

The area of an infinitesimal rectangle defined in a two-dimensional space or the volume of an infinitesimal cuboid defined in a three-dimensional space, where the vector $\mathrm{d}\boldsymbol{x}$ is the diagonal originating from the vertex $[x_1, \ldots, x_d]$, can be expressed as $d\tau = [\hat{\boldsymbol{x}}_1 \mathrm{d}x_1, \ldots, \hat{\boldsymbol{x}}_d \mathrm{d}x_d] = \prod_{i=1}^{d} \mathrm{d}x_i$. Here, for $d = 3$ the symbol $[\cdot, \cdot, \cdot]$ denotes the triple product of three vectors, whereas for $d = 2$, the symbol $[\cdot, \cdot]$ is the exterior product of two vectors. Note that in the other coordinate system, the corresponding infinitesimal element has the form

$$\begin{aligned} \mathrm{d}\tau' = \prod_{i=1}^{d} \mathrm{d}x_i &= \left[\frac{\partial \boldsymbol{x}}{\partial y_1} \mathrm{d}y_1, \ldots, \frac{\partial \boldsymbol{x}}{\partial y_d} \mathrm{d}y_d \right] \\ &= \mathcal{J}(y_1, \ldots, y_d) \prod_{i=1}^{d} \mathrm{d}y_i, \end{aligned} \tag{A2}$$

where

$$\mathcal{J}(y_1, \ldots, y_d) = \left[\frac{\partial \boldsymbol{x}}{\partial y_1}, \ldots, \frac{\partial \boldsymbol{x}}{\partial y_d} \right] = \left| \frac{\partial x_i}{\partial y_j} \right| \tag{A3}$$

is the Jacobian of the transformation from the former to the latter coordinate system. Performing a rotation of the former coordinate system one can make the versors $\hat{\boldsymbol{x}}_i$ overlap the versors $\hat{\boldsymbol{y}}_i$, and hence $\mathrm{d}\tau' = \mathrm{d}\tau = \prod_{i=1}^{d} \mathrm{d}x_i$. Since the Jacobian of the coordinate system rotation is always equal to 1, then according to the theorem for multiplication of determinants we state that the Jacobian, Eq. (A3), keeps its form. Moreover, the total symmetry of the problem under consideration ensures that for the inverse transformation (from the latter to the former coordinate system) Eq. (A2) must be of the form

$$\prod_{i=1}^{d} \mathrm{d}y_i = \mathcal{J}'(x_1, \ldots, x_d) \prod_{i=1}^{d} \mathrm{d}x_i,$$

where $\mathcal{J}'(x_1, \ldots, x_d) = \left| \frac{\partial y_i}{\partial x_j} \right|$, which allows us to conclude that the introduced Jacobians satisfy the relation

$$\mathcal{J}(y_1, \ldots, y_d) \mathcal{J}'(x_1, \ldots, x_d) = 1. \tag{A4}$$

On the other hand, taking into account that the new coordinate system is orthonormal and then including Eq. (A1) the Jacobian, Eq. (A3), reads

$$\begin{aligned} \mathcal{J}(y_1, \ldots, y_d) &= \left| \frac{\partial \boldsymbol{x}}{\partial y_1} \right| \cdot \ldots \cdot \left| \frac{\partial \boldsymbol{x}}{\partial y_d} \right| \\ &= \frac{1}{|\nabla_{\boldsymbol{x}} y_1| \cdot \ldots \cdot |\nabla_{\boldsymbol{x}} y_d|}. \end{aligned} \tag{A5}$$

Let us emphasize that the Jacobian of any transformation as well as the gradient of a function, in particular $|\nabla_{\boldsymbol{x}} y_i|$, are invariants of an orthogonal transformation. The infinitesimal translation vector originating from the vertex $[x_1, \ldots, x_d]$, which is the diagonal of the element $\mathrm{d}\tau$ can be written in the form $\mathrm{d}\boldsymbol{x} = \sum_{i=1}^{d} \hat{\boldsymbol{y}}_i \mathrm{d}x_i$. Then $\mathrm{d}y_i = \nabla_{\boldsymbol{x}} y_i \cdot \mathrm{d}\boldsymbol{x} = |\nabla_{\boldsymbol{x}} y_i| \mathrm{d}x_i$, and hence

$$\mathrm{d}x_i = \frac{\mathrm{d}y_i}{|\nabla_{\boldsymbol{x}} \mathrm{d}y_i|}. \tag{A6}$$

Employing jointly Eqs. (A2), (A5), and (A6) we obtain the formula

$$\mathcal{J}(y_1, \ldots, y_d) \prod_{i=1}^{d} \mathrm{d}y_i = \mathrm{d}y_1 \frac{\prod_{i=2}^{d} \mathrm{d}x_i}{|\nabla_{\boldsymbol{x}} y_1|}, \tag{A7}$$

where the differential elements $\mathrm{d}x_2$ or $\mathrm{d}x_2 \mathrm{d}x_3 = \mathrm{d}S$ belong to a curve or a surface perpendicular to the vector $\nabla_{\boldsymbol{x}} y_1$, respectively.

Consider the present discussion of the orthogonal momentum $\boldsymbol{k}$-space, for which the curvilinear, orthogonal transformation of the coordinate system is given, and where the first coordinate represents the one-particle energy spectrum ξ. By employing Eq. (A7), one can then state that the definitions of the density of states, for $d = 2$ or 3

$$\nu(\xi) = \frac{2}{(2\pi\hbar)^d} \int \frac{\prod_{i=2}^{d} \mathrm{d}k_i}{|\nabla_{\boldsymbol{k}} \xi|},$$

$$\nu(\xi) = \frac{2}{(2\pi\hbar)^d} \int \mathcal{J}(\xi, \ldots, \xi_d) \prod_{i=2}^{d} \mathrm{d}\xi_i$$

are quite equivalent. Here ξ_2, or ξ_2 and ξ_3 are the remaining coordinates of the used curvilinear system. Note that the integration in the former expression is taken over a one- or two-dimensional surface for the

fixed energy ξ, whereas the integration in the latter expression is taken over finite or infinite intervals of well-defined coordinates ξ_2, or ξ_2 and ξ_3, respectively, which can be chosen in any manner. To simplify the notation we define the kernel of the density of states as

$$\mathcal{K}(\xi,\ldots,\xi_d)=\frac{2}{(2\pi\hbar)^d}\mathcal{J}(\xi,\ldots,\xi_d). \tag{A8}$$

Then

$$\nu(\xi)=\int\mathcal{K}(\xi,\ldots,\xi_d)\prod_{i=2}^{d}\mathrm{d}\xi_i.$$

Appendix B: Basis functions of C_{4v} irreducible representations

The symmetry group of a square (in a 2D space), denoted C_{4v}, possesses one four-fold axis of symmetry, for which r defines a rotation by the angle $\pi/2$, and four planes of symmetry a, b, c, and d, which intersect at this axis. Hence, the group $C_{4v}=\{e,r,r^2,r^3,a,b,c,d\}$, where e is the identity element, possesses eight elements of symmetry as shown in Fig. 6. This is a non-abelian group. These elements can be separated into five equivalence classes, namely two single-element: $\{e\}$, $\{r^2\}$ and three two-element classes: $\{r,r^3\}$, $\{a,b\}$, $\{c,d\}$. This implies that the group C_{4v} possesses five irreducible representations, *i.e.,* four different one-dimensional ones and one 2D. Hence, there must always exist six basis functions gathered in four subsets containing one function: $\{f_1\}$, $\{f_2\}$, $\{f_3\}$, and $\{f_4\}$ and one subset containing two functions: $\{f_5 f_6\}$. These subsets are invariants of the group C_{4v}. Hence, the symmetry elements $\{e,r,r^2,r^3,a,b,c,d\}$ acting on the functions f_1,f_2,f_3,f_4 leave them unchanged (up to a sign), whereas acting on the functions f_5,f_6 they can form a linear combination of them. The properties of the invariant functions $\{f_i\}$, $i=1,2,3,4$ can be classified with reference to particular elements g of the group C_{4v} as follows:

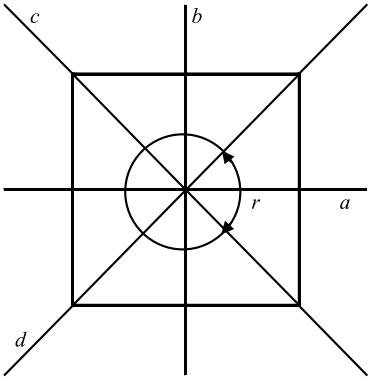

Fig. 6 Symmetry elements of a planar tetragonal system corresponding to the group C_{4v}.

i) The single-element subset $\{f_1\}$ of basis functions, corresponding to the trivial representation, such that $gf_1=f_1$ for all $g\in\{e,r,r^2,r^3,a,b,c,d\}$.

ii) The single-element subset $\{f_2\}$ of basis functions, corresponding to the representation with the trivial representation of the subgroup C_{2v}, such that $gf_2=f_2$ if $g\in\{e,r^2,a,b\}$ and $gf_2=-f_2$ if $g\in\{r,r^3,c,d\}$.

iii) The single-element subset $\{f_3\}$ of basis functions, corresponding to the representation with the trivial representation of another tetra-subgroup, such that $gf_3=f_3$ if $g\in\{e,r^2,c,d\}$ and $gf_3=-f_3$ if $g\in\{r,r^3,a,b\}$.

iv) The single-element subset $\{f_4\}$ of basis functions, corresponding to the representation with the trivial representation of the cyclic subgroup, such that $gf_4=f_4$ if $g\in\{e,r,r^2,r^3\}$ and $gf_4=-f_4$ if $g\in\{a,b,c,d\}$.

The properties of the invariant subset of basis functions $\{f_5,f_6\}$ corresponding to the 2D irreducible representation can be classified with reference to particular elements g of the group C_{4v} in one of the following two manners:

E$_s$ The two-element subset of the functions $\{f_5,f_6\}$ for the 2D representation:

$$gf_5=f_5 \text{ if } g\in\{e,a\},$$
$$gf_5=-f_5 \text{ if } g\in\{r^2,b\},$$
$$gf_5=-(-1)^s f_6 \text{ if } g\in\{r,d\},$$
$$gf_5=(-1)^s f_6 \text{ if } g\in\{r^3,c\},$$

and

$$gf_6=f_6 \text{ if } g\in\{e,b\},$$
$$gf_6=-f_6 \text{ if } g\in\{r^2,a\},$$
$$gf_6=-(-1)^s f_5 \text{ if } g\in\{r^3,d\},$$
$$gf_6=(-1)^s f_5 \text{ if } g\in\{r,c\},$$

where $s=1$ or 2. When the elements of the group C_{4v} act on a 2D momentum space with a Cartesian coordinate system, the components of the vector $\boldsymbol{k}=[k_x,k_y]$ are transformed as follows:

$$gk_x=k_x \text{ if } g\in\{e,a\},\quad gk_x=-k_x \text{ if } g\in\{r^2,b\},$$
$$gk_x=k_y \text{ if } g\in\{r,d\},\quad gk_x=-k_y \text{ if } g\in\{r^3,c\},$$

and

$$gk_y=k_y \text{ if } g\in\{e,b\},\quad gk_y=-k_y \text{ if } g\in\{r^2,a\},$$
$$gk_y=k_x \text{ if } g\in\{r^3,d\},\quad gk_y=-k_x \text{ if } g\in\{r,c\}.$$

The above relations allow us, after including the formula $gf_i(k_\alpha) = f_i(gk_\alpha)$, where $i = 1, 2, \ldots, 6$ and $\alpha = x$ or y, to choose invariant subsets of basis functions in accordance with the introduced classification in the form given by Eqs. (16)–(20). Since $g \cos k_x \cos k_y = \cos k_x \cos k_y$ for all $g \in C_{4v}$, one has the right to define invariant subsets of the basis functions as in Eqs. (21)–(25). Therefore, $g\xi_{\boldsymbol{k}} = \xi_{\boldsymbol{k}}$ for all $g \in C_{4v}$.

In the case of a polar coordinate system, the elements of the group C_{4v} acting on the angular coordinate φ transform it in the following manner

$$e\varphi = \varphi, \quad r\varphi = \varphi - \tfrac{\pi}{2}, \quad r^2\varphi = \varphi - \pi, \quad r^3\varphi = \varphi - \tfrac{3\pi}{2},$$
$$a\varphi = -\varphi, \quad b\varphi = \pi - \varphi, \quad c\varphi = \tfrac{3\pi}{2} - \varphi, \quad d\varphi = \tfrac{\pi}{2} - \varphi.$$

Hence, applying the formula $gf(\varphi) = f(g\varphi)$ to the Fourier harmonics, $1, \cos n\varphi, \sin n\varphi$, where $n = 1, 2, 3, \ldots$, we state that $g1 = 1$ for all $g \in C_{4v}$, and moreover

$$e\cos n\varphi = \cos n\varphi, \quad e\sin n\varphi = \sin n\varphi,$$
$$r\cos n\varphi = \begin{cases} (-1)^i \cos n\varphi & \text{if } n = 2i, \\ (-1)^i \sin n\varphi & \text{if } n = 1 + 2i, \end{cases}$$
$$r\sin n\varphi = \begin{cases} (-1)^i \sin n\varphi & \text{if } n = 2i, \\ -(-1)^i \cos n\varphi & \text{if } n = 1 + 2i, \end{cases}$$
$$r^2\cos n\varphi = (-1)^n \cos n\varphi, \quad r^2\sin n\varphi = (-1)^n \sin n\varphi,$$
$$r^3\cos n\varphi = \begin{cases} (-1)^i \cos n\varphi & \text{if } n = 2i, \\ -(-1)^i \sin n\varphi & \text{if } n = 1 + 2i, \end{cases}$$
$$r^3\sin n\varphi = \begin{cases} (-1)^i \sin n\varphi & \text{if } n = 2i, \\ (-1)^i \cos n\varphi & \text{if } n = 1 + 2i, \end{cases}$$
$$a\cos n\varphi = \cos n\varphi, \quad a\sin n\varphi = -\sin n\varphi,$$
$$b\cos n\varphi = (-1)^n \cos n\varphi, \quad b\sin n\varphi = -(-1)^n \sin n\varphi,$$
$$c\cos n\varphi = \begin{cases} (-1)^i \cos n\varphi & \text{if } n = 2i, \\ -(-1)^i \sin n\varphi & \text{if } n = 1 + 2i, \end{cases}$$
$$c\sin n\varphi = \begin{cases} -(-1)^i \sin n\varphi & \text{if } n = 2i, \\ -(-1)^i \cos n\varphi & \text{if } n = 1 + 2i, \end{cases}$$
$$d\cos n\varphi = \begin{cases} (-1)^i \cos n\varphi & \text{if } n = 2i, \\ (-1)^i \sin n\varphi & \text{if } n = 1 + 2i, \end{cases}$$
$$d\sin n\varphi = \begin{cases} -(-1)^i \sin n\varphi & \text{if } n = 2i, \\ (-1)^i \cos n\varphi & \text{if } n = 1 + 2i, \end{cases}$$

where $i = 0, 1, 2, \ldots$. These relations allow us to perform the following classification of the functions 1, $\cos n\varphi$, and $\sin n\varphi$:

i) The functions 1 and $\cos 4i\varphi$, $i = 1, 2, 3, \ldots$, are invariants and each of them has the same properties as the function f_1 of subset A.

ii) The functions $\sin 4i\varphi$, $i = 1, 2, 3, \ldots$, are invariants and each of them has the same properties as the function f_4 of subset D.

iii) The functions $\cos(1 + 4i)\varphi$ and $\sin(1 + 4i)\varphi$, for a fixed $i = 0, 1, 2, \ldots$, have the same properties as the functions f_5 and f_6, respectively, of the invariable subset E_1.

iv) The functions $\cos(2 + 4i)\varphi$, $i = 0, 1, 2, \ldots$, are invariants and each of them has the same properties as the function f_2 of subset B.

v) The functions $\sin(2 + 4i)\varphi$, $i = 0, 1, 2, \ldots$, are invariants and each of them has the same properties as the function f_3 of subset C.

vi) The functions $\cos(3 + 4i)\varphi$ and $\sin(3 + 4i)\varphi$, for a fixed $i = 0, 1, 2, \ldots$, have the same properties as the functions f_5 and f_6, respectively, of the invariable subset E_2.

Thus, all Fourier harmonics, 1, $\cos n\varphi$, and $\sin n\varphi$, can be collected in only five possible types of invariant subsets.

Appendix C: Symmetry properties of separable parts of pairing interactions

The separated parts of the pairing interactions (14) and (15) have the following symmetry properties with regard to elements of the group C_{4v}:

i) The functions 1 and $\cos k_x + \cos k_y$ are invariants and they have the same properties as the function f_1 of subset A,

ii) The function $\cos k_x - \cos k_y$ is an invariant and it has the same properties as the function f_2 of subset B,

iii) The functions $\sin k_x$ and $\sin k_y$, have the same properties as the functions f_5 and f_6, respectively, of the invariant subset E_1.

The corresponding functions of φ in the pairing potential must have the same symmetry properties. Note that the function $f(\varphi)$ defined by Eq. (28), which is of the form

$$f(\varphi) = \frac{|\sin\varphi| - |\cos\varphi|}{|\sin\varphi| + |\cos\varphi|},$$

when $0 \leq \varphi < 2\pi$, has the same properties as function f_2 of subset B. Hence, $gX(\xi, \varphi) = X(\xi, \varphi)$ if $g \in \{e, r^2, a, b\}$, $gX(\xi, \varphi) = Y(\xi, \varphi)$ if $g \in \{r, r^3, c, d\}$, $gY(\xi, \varphi) = Y(\xi, \varphi)$ if $g \in \{e, r^2, a, b\}$, and $gY(\xi, \varphi) = X(\xi, \varphi)$ if $g \in \{r, r^3, c, d\}$. This implies that

i′) The function $[X(\xi, \varphi, \eta) + Y(\xi, \varphi, \eta) - 2]/2\eta$ is an

invariant and has the same properties as the function f_1 of subset A,

ii′) and the function $[Y(\xi,\varphi,\eta)-X(\xi,\varphi,\eta)]/2\eta$ is an invariant and has the same properties as the function f_2 of subset B.

iii′) Moreover, the functions

$$(\pm)\frac{1}{2\eta}\sqrt{\eta^2-[X(\xi,\varphi,\eta)-1]^2}$$

and

$$(\pm)\frac{1}{2\eta}\sqrt{\eta^2-[Y(\xi,\varphi,\eta)-1]^2}$$

have the same properties as the functions f_5 and f_6 of the invariant subset E_1, respectively or, conversely, as the functions f_6 and f_5 of the invariant subset E_1, respectively, where the sign + or − must be chosen for an appropriate quadrant of the Cartesian coordinate system in the momentum space, in accordance with the sign of the functions $\sin k_x$ and $\sin k_y$.

Since the applied conformal transformation is based on a solution of the differential equation, which is formulated based on a particular dispersion relation, the obtained solutions should be properly symmetrized to correspond with the symmetry of the dispersion relation $\xi_{\boldsymbol{k}}$. Taking into account the properties of $X(\xi,\varphi)$ and $Y(\xi,\varphi)$, discussed above, we state that

$$g\left[\frac{1}{2\eta}\sqrt{\eta^2-[X(\xi,\varphi)-1]^2}+\frac{1}{2\eta}\sqrt{\eta^2-[Y(\xi,\varphi)-1]^2}\right]$$
$$=\frac{1}{2\eta}\sqrt{\eta^2-[X(\xi,\varphi)-1]^2}+\frac{1}{2\eta}\sqrt{\eta^2-[Y(\xi,\varphi)-1]^2}$$

for all $g\in C_{4v}$. Thus, this function is invariant in the subset E_1.

The obtained relations and the classification of the Fourier harmonics performed in B prove that the Fourier expansions of the specified functions must have the following forms

$$\frac{1}{2\eta}\left[X(\xi,\varphi,\eta)+Y(\xi,\varphi,\eta)-2\right]$$
$$=\frac{\chi_0(\xi,\eta)}{\sqrt{2}}+\sum_{l=1}^{\infty}\chi_{4l}(\xi,\eta)\cos 4l\varphi,$$

where

$$\chi_0(\xi,\eta)=\frac{\sqrt{2}}{\eta\pi}\int_0^{\pi/2}\left[X(\xi,\varphi,\eta)+Y(\xi,\varphi,\eta)-2\right]\mathrm{d}\varphi$$

and

$$\chi_{4l}(\xi,\eta)=\frac{2}{\eta\pi}\int_0^{\pi/2}\left[X(\xi,\varphi,\eta)+Y(\xi,\varphi,\eta)-2\right]$$
$$\times\cos 4l\varphi\mathrm{d}\varphi$$

for $l=1,2,\ldots$, and

$$\frac{1}{2\eta}\left[Y(\xi,\varphi,\eta)-X(\xi,\varphi,\eta)\right]$$
$$=\sum_{l=0}^{\infty}\chi_{2+4l}(\xi,\eta)\cos(2+4l)\varphi.$$

Here

$$\chi_{2+4l}(\xi,\eta)=\frac{2}{\eta\pi}\int_0^{\pi/2}\left[Y(\xi,\varphi,\eta)-X(\xi,\varphi,\eta)\right]$$
$$\times\cos(2+4l)\varphi\mathrm{d}\varphi,$$

$$(\pm)\frac{\sqrt{2}}{4\eta}\left\{\sqrt{\eta^2-[X(\xi,\varphi)-1]^2}+\sqrt{\eta^2-[Y(\xi,\varphi)-1]^2}\right\}$$
$$=\sum_{l=0}^{\infty}\chi_{1+4l}(\xi,\eta)\cos(1+4l)\varphi,$$

and

$$(\pm)\frac{\sqrt{2}}{4\eta}\left\{\sqrt{\eta^2-[X(\xi,\varphi)-1]^2}+\sqrt{\eta^2-[Y(\xi,\varphi)-1]^2}\right\}$$
$$=\sum_{l=0}^{\infty}\chi_{1+4l}(\xi,\eta)\sin(1+4l)\varphi,$$

where

$$\chi_{1+4l}(\xi,\eta)=\frac{\sqrt{2}}{\eta\pi}\int_0^{\pi/2}\left\{\sqrt{\eta^2-[X(\xi,\varphi)-1]^2}\right.$$
$$\left.+\sqrt{\eta^2-[Y(\xi,\varphi)-1]^2}\right\}\cos(1+4l)\varphi\mathrm{d}\varphi$$
$$=\frac{\sqrt{2}}{\eta\pi}\int_0^{\pi/2}\left\{\sqrt{\eta^2-[X(\xi,\varphi)-1]^2}\right.$$
$$\left.+\sqrt{\eta^2-[Y(\xi,\varphi)-1]^2}\right\}\sin(1+4l)\varphi\mathrm{d}\varphi$$

for $l=0,1,2,\ldots$, where the latter coefficients are symmetrized to be invariants with respect to the choice of $X(\xi,\varphi,\eta)$ and $Y(\xi,\varphi,\eta)$ [10–12].

References

1. P. Monthoux and G. G. Lonzarich, p-wave and d-wave superconductivity in quasi-two-dimensional metals, *Phys. Rev. B* 59(22), 14598 (1999)
2. P. Monthoux and G. G. Lonzarich, Magnetically mediated superconductivity in quasi-two and three dimensions, *Phys. Rev. B* 63(5), 054529 (2001)
3. P. Monthoux and G. G. Lonzarich, Magnetically mediated superconductivity: Crossover from cubic to tetragonal lattice, *Phys. Rev. B* 66(22), 224504 (2002)

4. A. Nazarenko and E. Dagotto, Possible phononic mechanism for d_{x2y2} superconductivity in the presence of short-range antiferromagnetic correlations, *Phys. Rev. B* 53(6), R2987 (1996)
5. D. Y. Xing, M. Liu, Y. G. Wang, and J. Dong, Analytic approach to the antiferromagnetic van Hove singularity model for high-T_c superconductors, *Phys. Rev. B* 60(13), 9775 (1999)
6. M. R. Norman and C. Pépin, The electronic nature of high temperature cuprate superconductors, *Rep. Prog. Phys.* 66(10), 1547 (2003)
7. R. Gonczarek, M. G ladysiewicz-Kudrawiec, The Van Hove Scenario in high-T_c superconductivity, Wrocław University of Technology Press, Wrocław, 2004 (in Polish)
8. R. Gonczarek and M. Krzyzosiak, Conformal transformation method and symmetry aspects of the group C_{4v} in a model of high-T_c superconductors with anisotropic gap, *Physica C* 426(431), 278 (2005)
9. R. Gonczarek, L. Jacak, M. Krzyzosiak, and A. Gonczarek, Competition mechanism between singlet and triplet superconductivity in the tight-binding model with anisotropic attractive potential, *Eur. Phys. J. B* 49(2), 171 (2006)
10. R. Gonczarek, M. Krzyzosiak, L. Jacak, andA. Gonczarek, Coexistence of spin-singlet *s*- and *d*-wave and spin-triplet *p*-wave order parameters in anisotropic superconductors, *phys. stat. sol. (b)* 244, 3559 (2007)
11. R. Gonczarek, M. Krzyzosiak, and A. Gonczarek, Islands of stability of the *d*-wave order parameter in *s*-wave anisotropic superconductors, *Eur. Phys. J. B* 61(3), 299 (2008)
12. M. Krzyzosiak, R. Gonczarek, A. Gonczarek, and L. Jacak, Interplay between spin-singlet and spin-triplet order parameters in a model of an anisotropic superconductor with cuprate planes, *J. Phys. Conf. Ser.* 152, 012057 (2009)
13. R. Szczęśniak and A. P. Durajski, The characterization of high-pressure superconducting state in Si_2H_6 compound: The strong-coupling description, *J. Phys. Chem. Solids* 74(4), 641 (2013)
14. R. Szczęśniak, SDW antiferromagnetic phase in the two-dimensional Hubbard model: Eliashberg approach, *Phys. Lett. A* 373(4), 473 (2009)
15. W. Kohn and J. M. Luttinger, New mechanism for superconductivity, *Phys. Rev. Lett.* 15(12), 524 (1965)
16. Y. A. Krotov, D. H. Lee, and A. V. Balatsky, Superconductivity of a metallic stripe embedded in an antiferromagnet, *Phys. Rev. B* 56(13), 8367 (1999)
17. M. Granath and H. Johannesson, One-dimensional electron liquid in an antiferromagnetic environment: Spin gap from magnetic correlations, *Phys. Rev. Lett.* 83(1), 199 (1999)
18. A. P. Durajski and R. Szczęśniak, Characterization of phonon-mediated superconductivity in lithium doping borocarbide, *Solid State Sci.* 42, 20 (2015)
19. A. P. Durajski, Phonon-mediated superconductivity in compressed NbH_4 compound, *Eur. Phys. J. B* 87(9), 210 (2014)
20. P. W. Anderson, The resonating valence bond state in La_2CuO_4 and superconductivity, *Science* 235(4793), 1196 (1987)
21. P. W. Anderson, The Theory of High-T_c Superconductivity in the Cuprates, Princeton University Press, 1997
22. L. D. Landau, The Theory of a Fermi Liquid, *Zh. Eksp. Teor. Fiz.* 80, 1058 (1956) [*Sov. Phys. JETP* 3, 920 (1956)]
23. L. D. Landau, Oscillations in a Fermi liquid, *Zh. Eksp. Teor. Fiz.* 32, 59 (1957) [*Sov. Phys. JETP* 5, 101(1957)]
24. M. Krzyzosiak, R. Gonczarek, A. Gonczarek, and L. Jacak, Conformal Transformation Method in Studies of High-T_c Superconductors — Beyond the Van Hove Scenario, in: Superconductivity and Superconducting Wires, edited by D. Matteri and L. Futino, Nova Science Publishers, 2010, Ch. 5
25. R. Gonczarek, M. Krzyzosiak, and M. Mulak, Valuation of characteristic ratios for high-T_c superconductors with anisotropic gap in the conformal transformation method, *J. Phys. A* 37(18), 4899 (2004)
26. R. Gonczarek, M. Gładysiewicz, and M. Mulak, On possible formalism of anisotropic Fermi liquid and BCS-type superconductivity, *Int. J. Mod. Phys. B* 15(05), 491 (2001)
27. F. C. Zhang and T. M. Rice, Effective Hamiltonian for the superconducting Cu oxides, *Phys. Rev. B* 37(7), 3759 (1988)
28. R. Micnas, J. Ranniger, and S. Robaszkiewicz, Superconductivity in narrow-band systems with local nonretarded attractive interactions, *Rev. Mod. Phys.* 62(1), 113 (1990)
29. E. Pavarini, I. Dasgupta, T. Saha-Dasgupta, O. Jepsen, and O. K. Andersen, Band-structure trend in hole-doped cuprates and correlation with T_{rmcmax}, *Phys. Rev. Lett.* 87(4), 047003 (2001)
30. O. K. Andersen, A. I. Liechtenstein, O. Jepsen, and F. Paulsen, LDA energy bands, low-energy hamiltonians, t', t'', $t(k)$, and J, *J. Phys. Chem. Solids* 56(12), 1573 (1995)
31. O. K. Andersen, S. Y. Savrasov, O. Jepsen, and A. I. Liechtenstein, Out-of-plane instability and electron-phonon contribution to *s*- and *d*-wave pairing in high-temperature superconductors; LDA linear-response calculation for doped $CaCuO_2$ and a generic tight-binding model *J. Low Temp. Phys.* 105(3–4), 285 (1996)
32. R. Gonczarek, M. G. ladysiewicz, and M. Mulak, Equilibrium states and thermodynamical properties of *d*-wave paired HTSC in the tightbinding model, *phys. stat. sol. (b)* 233, 351 (2002)
33. M. M. Maśka, M. Mierzejewski, B. Andrzejewski, M. L. Foo, R. J. Cava, and T. Klimczuk, Possible singlet-to-triplet pairing transition in $Na_xCoO_{2-y}H_2O$, *Phys. Rev. B* 70, 144516 (2004)
34. J. Bouvier and J. Bok, The Gap Symmetry and Fluctuations in High T_c Superconductors, Eds. J. Bok, G.

Deutscher, D. Pavuna, and S. Wolf, New York: Plenum Press, 1998, p. 37

35. R. S. Markiewicz, A survey of the Van Hove scenario for high-$T_c$superconductivity with special emphasis on pseudogaps and striped phases, *J. Phys. Chem. Solids* 58(8), 1179 (1997)
36. H. Q. Lin and J. E. Hirsch, Two-dimensional Hubbard model with nearest- and next-nearest-neighbor hopping, *Phys. Rev. B* 35(7), 3359 (1987)
37. M. Sigist and K. Ueda, Phenomenological theory of unconventional superconductivity, *Rev. Mod. Phys.* 63(2), 239 (1991)
38. H. Ghosh, Higher anisotropic d-wave symmetry in cuprate superconductors, *J. Phys.: Condens. Matter* 11(30), L371 (1999)
39. Q. Yuan and P. Thalmeier, BCS theory for $s+g$-wave superconductivity in borocarbides Y(Lu)Ni_2B_2C, *Phys. Rev. B*68(17), 174501 (2003)
40. H. Shimahara and S. Hata, Superconductivity in a ferromagnetic layered compound, *Phys. Rev. B* 62(21), 14541 (2000)
41. J. González, Microscopic description of d-wave superconductivity by Van Hove nesting in the Hubbard model, *Phys. Rev. B* 63(2), 024502 (2000)
42. E. Ya. Sherman, Raman vertex in cuprates: Role of the extended Van Hove singularity, *Phys. Rev. B* 58(21), 14187 (1998)
43. R. Gonczarek and M. Krzyzosiak, On possibility of realization of d- or p-wave symmetry states in anisotropic superconductors, *Acta Phys. Pol. A* 109(4–5), 493 (2006)
44. R. Gonczarek and M. Krzyzosiak, On a model of superconductivity realized in the metallic phase of strongly correlated electrons revealing a first-order phase transition, *Int. J. Mod. Phys. B* 17(30), 5683 (2003)
45. R. Gonczarek and M. Krzyzosiak, Critical parameters in the superconducting singular Fermi liquid model, *Physica C* 445–448, 158 (2006)
46. A. P. Durajski, The anisotropic evolution of the energy gap in Bi2212 superconductor, *Front. Phys.* 11, 117408 (2016)
47. C. C. Tsuei, D. M. Newns, C. C. Chi, and P. C. Pattnaik, Anomalous isotope effect and Van Hove singularity in superconducting Cu oxides, *Phys. Rev. Lett.* 65(21), 2724 (1990)
48. C. C. Tsuei, D. M. Newns, C. C. Chi, and P. C. Pattnaik, Tsuei *et al.* reply, *Phys. Rev. Lett.* 68(7), 1091 (1992)
49. E. Dagotto, A. Nazarenko, and M. Boninsegni, Flat quasiparticle dispersion in the 2D t–J model, *Phys. Rev. Lett.* 73(5), 728 (1994)
50. E. Dagotto, Correlated electrons in high-temperature superconductors, *Rev. Mod. Phys.* 66(3), 763 (1994)
51. E. Dagotto, A. Nazarenko, and A. Moreo, Antiferromagnetic and van Hove scenarios for the cuprates: Taking the best of both worlds, *Phys. Rev. Lett.* 74(2), 310 (1995)
52. J. M. Getino, M. de Llano, and H. Rubio, Properties of the gap energy in the van Hove scenario of high-temperature superconductivity, *Phys. Rev. B* 48(1), 597 (1993)
53. R. S. Markiewicz, Van Hove excitons and high-T_c superconductivity (VI): Properties of the exitations, *Physica C* 168(1–2), 195 (1990)
54. R. S. Markiewicz, Van Hove excitons and high-T_c superconductivity (VI): Gap equation with pair breaking, *Physica C* 183, 303 (1991)
55. R. S. Markiewicz, C. Kusko, and V. Kidambi, Pinned Balseiro-Falicov model of tunneling and photoemission in the cuprates, *Phys. Rev. B* 60(1), 627 (1999)
56. H. H. Fertwell, A. Kaminski, J. Mesot, J. C. Campuzano, M. R. Norman, M. Randeria, T. Sato, R. Gatt, T. Takahashi and K. Kadowaki, Fermi surface of $Bi_2Sr_2CaCu_2O_8$, *Phys. Rev. Lett.* 84(19), 4449 (2000)
57. S. V. Borisenko, M. S. Golden, S. Legner, T. Pichler, C. Dürr, M. Knupfer, J. Fink, G. Yang, S. Abell, and H. Berger, Joys and pitfalls of Fermi surface mapping in $Bi_2Sr_2CaCu_2O_{8+\delta}$ using angle resolved photoemission, *Phys. Rev. Lett.* 84(19), 4453 (2000)
58. K. Kuboki, Effect of band structure on the symmetry of superconducting states, *J. Phys. Soc. Jpn.* 70(9), 2698 (2001)
59. R. Gonczarek and M. Krzyzosiak, Some universal relations between the gap and thermodynamic functions plausible for various models of superconductors, *phys. stat. sol. (b)* 238, 29 (2003)
60. R. Gonczarek and M. Mulak, Enhancement of critical temperature of superconductors implied by the local fluctuation of EDOS, *Phys. Lett. A* 251(4), 262 (1999)